Gravitational radiation from inspiralling compact binaries to N^{3}LO in the effective field theory approach

Loris Amalberti,[1,2,*] Zixin Yang,[1,†] and Rafael A. Porto[1,‡]

[1]*Deutsches Elektronen-Synchrotron DESY, Notkestrasse 85, 22607 Hamburg, Germany*
[2]*Institut für Physik, Humboldt-Universität zu Berlin, 12489 Berlin, Germany*

(Received 15 June 2024; accepted 23 July 2024; published 23 August 2024)

Within the context of the effective field theory (EFT) framework to gravitational dynamics, we compute the Hamiltonian, source quadrupole moment, and gravitational-wave energy flux for (nonspinning) inspiralling compact binaries at next-to-next-to-next-to leading order (N^{3}LO) in the post-Newtonian (PN) expansion. We use the recently developed d-dimensional multipole-expanded effective theory, and explicitly perform the matching to the (pseudo) stress-energy tensor. The calculation involves Feynman integrals up to three- (conservative) and two-loop (radiative) orders, evaluated within dimensional regularization. Our (ambiguity-free) results confirm (for the first time) the value of the gravitational-wave flux for quasicircular orbits at 3PN order, while paving the way forward to the inclusion of spin effects as well as higher-order computations.

DOI: 10.1103/PhysRevD.110.044046

I. INTRODUCTION

The LIGO-Virgo-KAGRA Collaboration has observed $\mathcal{O}(10^2)$ gravitational-wave (GW) signals from binary compact objects [1], including some that have been found, e.g., [2,3], analyzing the publicly available data [4]. Future detectors such as the Laser Interferometer Space Antenna (LISA) [5], Cosmic Explorer (CE) [6], and the Einstein Telescope (ET) [7,8], are expected to significantly increase the detection rates. The sheer number of new sources that will be accessible to third-generation GW observatories thus highlights the necessity of establishing high-precision analytic waveform templates for binary searches, not only for detection but more importantly to extract accurate physical information regarding the wave's origin (see, e.g., [9] for the case of LISA sources).

In this paper we focus on the (weak-field and slow-velocity) post-Newtonian (PN) expansion of the two-body problem in gravity, e.g., [10–15], and in particular the effective field theory (EFT) approach to gravitational dynamics [16–26]. In the realm of the PN approximation, the current state of the art for nonspinning bodies is the 4.5PN precision for the phase [27] [i.e., the $(v/c)^9$ correction to the leading order], the 4PN order for both the GW flux and the dominant quadrupolar amplitude mode [28] and 3.5PN for the subleading ones [29–31]. For the case of spinning bodies, on the other hand, the state of the art is at 4PN for the GW flux [32,33] and to 3.5PN order for the amplitude [34–36], as well as 4.5PN in the radiation-reaction force [37,38]. Although, overall the EFT approach has achieved the most accurate description of the dynamics for spinning bodies [32–34,37–39], as well as in the *conservative* sector for nonspinning binaries, with partial results to next^5-to-leading order (N^{5}LO) [40–48], the computation of the GW energy flux has been performed only to N^{2}LO so far, namely at 2PN (and 4PN) order for nonspinning (spinning) compact objects, respectively [32,33,49]. The purpose of this paper is to report on the derivation of the (nonspinning) GW flux at N^{3}LO within the EFT approach. As we shall see, our (ambiguity-free) results agree with what had been—up until only a year ago [28]—one of the key ingredients for the state of the art in the modeling of binary compact objects in gravity [50–52],[1] thus paving the road forward to including spin effects to a similar N^{3}LO level of accuracy, as well as higher order computations.

There are several conceptual and computational issues that start to appear at N^{3}LO. Notably, the well-known UV divergences in both the equations of motion [25] and nonlinear radiative corrections [22]. Dimensional regularization (dim. reg.), a method extensively employed in the EFT framework since the seminal work in [16] (see also [53,54]), has become the weapon of choice to tackle divergent terms, appearing as poles $\propto (d-3)^{-1}$ (with d the number of spatial dimensions), naturally yielding results which are devoid of the ambiguities that polluted the

*Contact author: loris.amalberti@desy.de
†Contact author: zixin.yang@desy.de
‡Contact author: rafael.porto@desy.de

[1]To our knowledge, this is the first confirmation of the source GW flux obtained in [50,51] at 3PN order, which had not been reproduced by an independent methodology until now.

previous derivation [50–52]. While the ambiguity-free nature of the EFT approach, dealing with not only UV but also IR divergences, has already been demonstrated for the conservative sector up to 4PN order [40–42], the computation of the GW flux necessitates an equally careful examination of divergent terms as well as of the multipole expansion at the level of the action in d-dimensions, a subject only recently studied in [55]. After including all contributions form the source multipole moments, as well as hereditary effects [22], the final result for the total radiated energy is devoid of singularities, as expected, and produces a radiated GW flux for quasicircular orbits which is in perfect agreement with the original result in [50,51]. The application of the steps described in this paper to incorporate spin effects up to 5PN order will be reported elsewhere.

This paper is organized as follows. A brief summary of the EFT approach is provided in Sec. II. An independent derivation of the conservative dynamics to N^{3}LO is offered in Sec. III, while the contributions to the radiative multipole moments through a matching computation, the total radiated power, and radiated energy for quasicircular orbits, are discussed in Sec. IV. We conclude in Sec. V. Useful formulas are collected in Appendix A, while other known contributions to the (lower order) multipoles are presented in Appendix B, alongside various consistency checks. All our computations are performed with the help of the software `Mathematica` and various associated packages, `FeynArts` [56], `xAct` [57] (including subpackages `xTensor` and `xPert`), as well as the integration-by-parts (IBP) program `LiteRed` [58]. A computer-readable ancillary file detailing various results presented here is included with the submission of this paper [59].

Notation: We use $\hbar = c = 1$ units with the mostly negative metric convention. In the context of dim. reg., we work in $d+1$ spacetime dimensions, with one time and d spatial dimensions. Greek letters denote Lorentz indices (running from 0 to d), and Latin letters the spatial ones (running from 1 to d). Bold symbols denote spatial vectors, and we define the relative position, $\mathbf{r} \equiv \mathbf{x}_1 - \mathbf{x}_2$, the relative velocity, $\mathbf{v} \equiv \mathbf{v}_1 - \mathbf{v}_2$ and relative acceleration, $\mathbf{a} \equiv \mathbf{a}_1 - \mathbf{a}_2$, respectively. We follow the standard definitions $M \equiv m_1 + m_2$, $\nu \equiv m_1 m_2/M^2$, $\Delta = (m_1 - m_2)/M = \sqrt{1-4\nu}$, and $m_{\rm Pl} \equiv 1/\sqrt{32\pi G}$, for the total mass, symmetric mass ratio, mass difference, and Planck's mass, respectively. Finally, we use $\int \mathrm{d}^d\mathbf{q}/(2\pi)^d \equiv \int_{\mathbf{q}}$ for the integration measure, and follow the multi-index notation introduced in [60], i.e., $x^L \equiv x^{i_1}x^{i_2}\ldots x^{i_{\ell-1}}x^{i_\ell}$ and $I^L \equiv I^{i_1 i_2 \ldots i_{\ell-1} i_\ell}$, for the coordinates and multipole moments, respectively.

II. EFFECTIVE FIELD THEORY SETUP

In this section we give a brief overview of the EFT approach and point the reader to the reviews in [13–15], as well as the previous N^{2}LO derivation in [49], for more details. The inspiral dynamics of compact binaries can be delineated across three distinct length scales; the characteristic size of the bodies, $r_s \sim GM$, the orbital separation between them, r, and the wavelength of the gravitational radiation, $\lambda_{\rm GW}$. In the PN regime of small velocities, $v \ll 1$, these length scales form an intertwined hierarchical structure,

$$r_s \ll r \ll \lambda_{\rm GW}, \tag{2.1}$$

which enables us to disentangle distinct physical effects from different scales in terms of a unified expansion parameter, v, thus facilitating the computations of GW observables. After integrating-out (solving-for) the short-distance scale of each compact body (r_s), the object is described in terms of a worldline point-particle action, $S_{\rm pp}$, which for our purposes can be written as ($a = 1, 2$)

$$\begin{aligned} S_{\rm pp} &= \sum_a m_a \int d\tau_a + \cdots \\ &= \sum_a m_a \int \sqrt{g_{\mu\nu} v_a^\mu v_a^\nu}\, d\sigma_a + \cdots, \end{aligned} \tag{2.2}$$

where $v_a^\mu \equiv \frac{dx_a^\mu}{d\sigma_a}$, with σ_a an affine parameter. The ellipses include spin as well as higher-order finite-size effects. In this paper we consider Einstein's gravity, described by the Einstein-Hilbert action,

$$S_{\rm EH} = -2m_{\rm Pl}^2 \int \mathrm{d}^4x \sqrt{-g} R[g], \tag{2.3}$$

with $R[g]$ the Riemann curvature scalar. In the scenario in (2.1), one can split the gravitational field into separate, nonoverlapping regions, via [16,61]

$$g_{\mu\nu} = \eta_{\mu\nu} + \frac{h_{\mu\nu}(x)}{m_{\rm Pl}} = \eta_{\mu\nu} + \frac{\bar{h}_{\mu\nu}(x)}{m_{\rm Pl}} + \frac{H_{\mu\nu}(x)}{m_{\rm Pl}}, \tag{2.4}$$

with $\eta_{\mu\nu}$ the Minkowski metric. The (off shell) potential modes, responsible for the binding of the system, are denoted as $H_{\mu\nu}$, whereas the (on shell) radiation modes, describing the GW emission, are $\bar{h}_{\mu\nu}$, respectively; obeying the following scaling rules [16]:

$$\partial_0 H_{\mu\nu} \sim \left(\frac{v}{r}\right), \quad \partial_i H_{\mu\nu} \sim \left(\frac{1}{r}\right), \quad \partial_\alpha \bar{h}_{\mu\nu} \sim \left(\frac{v}{r}\right). \tag{2.5}$$

The dynamics of the system is obtained after integrating out both the potential and radiation modes in the effective theory, one scale at the time. For instance, up to 3PN order, the effective gravitational potential, $V[x_a]$, from which we can obtain the binding energy, may be obtained via

$$e^{-i\int dtV[x_a]} = \int DH_{\mu\nu} e^{iS_{\rm EH}[H]+iS_{\rm GF}^{(\bar{h}=0)}[H]+iS_{\rm pp}[x_a,H]}, \quad (2.6)$$

ignoring the radiation fields and using the standard harmonic gauge-fixing condition, $S_{\rm GF}^{(\bar{h}=0)} \propto (\partial_\alpha H^\alpha_\mu - \frac{1}{2}\partial_\mu H^\alpha_\alpha)^2$. For the sake of completeness, we derive the conservative effects at N^{3}LO [51], first rederived within the EFT approach in [25], but we do so using different metric variables and gauge condition.

For the derivation of radiative effects, on the other hand, we perform a matching computation. This is achieved by integrating out the potential modes in the *full theory*, including both H and $\bar{h}$ fields, and reading off the (time-dependent) mass- (I^L) and current-type (J^L) couplings in the multipole-expanded effective theory [22,26], recently constructed in d dimensions in [55]. The long-distance effective action takes the form, schematically,[2]

$$S_{\rm eff} = \frac{1}{2}\int dt (I^L(t)\partial_{L-2}E_{i_{\ell-1}i_\ell} + J^L(t)\partial_{L-2}B_{i_{\ell-1}i_\ell}), \quad (2.7)$$

in terms of the electric, E, and magnetic, B, components of the Weyl tensor, which follows from a multipole expansion (around the binary's center-of-mass) of the linearized coupling,

$$\frac{1}{2m_{\rm Pl}}\int {\rm d}^d x T^{\mu\nu}\bar{h}_{\mu\nu}, \quad (2.8)$$

with $T^{\mu\nu}$ the (pseudo)stress-energy tensor. See [22,26,55] for details. Crucially, the matching computation is performed using a background-field gauge for the potential modes,

$$S_{\rm GF}^{(\bar{h})} = m_{\rm Pl}^2 \int {\rm d}^4 x \sqrt{\bar{g}}\Gamma_\mu\Gamma^\mu, \quad (2.9)$$

where $\Gamma_\mu = D_\alpha H^\alpha_\mu - \frac{1}{2}D_\mu H^\alpha_\alpha$, using the covariant derivative associated to the (background) radiation field $\bar{g}_{\mu\nu}$. This ensures that the resulting $T^{\mu\nu}$ obeys the Ward identity, $\partial_\mu T^{\mu\nu} = 0$, which is required for the construction of the (gauge-invariant) effective theory.

[2]Formally speaking, the J^L coupling in (2.7) only exists in $d = 3$ dimensions, and it must be extended to a generalized coupling to the curvature tensor for $d \neq 3$. Moreover, an extra (Weyl-type) multipole moment appears, which vanishes for $d = 3$. (See [55] for details.) Although, crucially, the d-dimensional expressions for the (I^L, J^L) in terms of moments of the stress-energy tensor are needed, none of the subtleties associated with additional couplings play a role at N^{3}LO order, and first appear at 4PN [27].

III. CONSERVATIVE DYNAMICS AT N^{3}LO

We start by rederiving the conservative part of the dynamics of the binary system at 3PN order, which will be needed to derive the equations of motion entering in the GW flux. Moreover, since it is actually inconsequential in the radiation sector, we perform this computation without resorting to a further decomposition of the gravitational field into polarization modes [25], thus providing yet another independent check of the results. For the computation of the gravitational potential, we only require the (instantaneous) propagator for potential modes, with the structure,

$$-iP_{\mu\nu;\alpha\beta}\delta(t)\int_{\mathbf{q}}\frac{1}{\mathbf{q}^2}e^{i\mathbf{q}\cdot\mathbf{x}}, \quad (3.1)$$

where $P_{\mu\nu;\alpha\beta} = \frac{1}{2}[\eta_{\mu\alpha}\eta_{\nu\beta} + \eta_{\mu\beta}\eta_{\nu\alpha} - \frac{2}{d-1}\eta_{\mu\nu}\eta_{\alpha\beta}]$. We display in Fig. 1 a representative set of Feynman topologies, entering at $\mathcal{O}(G^4)$, with the dashed lines representing the propagator of potential modes and the solid lines representing the (nonpropagating) worldlines, treated as external sources. See Appendix A for additional terms, including those responsible for departures from instantaneity, see also Appendix B 1 for various other contributions.

We employ the IBP program `LiteRed` to facilitate the reduction of the integrand families into a smaller collection of independent set of ("three-loop") Feynman master integrals, which we evaluate in dim. reg., yielding

$$M_{3,1} = \int_{\mathbf{q}_1,\mathbf{q}_2,\mathbf{q}_3}\frac{1}{\mathbf{q}_1^2(\mathbf{q}_1-\mathbf{q}_2)^2(\mathbf{q}_2+\mathbf{q}_3)^2(\mathbf{q}_3-\mathbf{p})^2} = \frac{|\mathbf{p}|^{-8+3d}}{(4\pi)^{\frac{3d}{2}}}\frac{\Gamma(4-\frac{3d}{2})\Gamma(\frac{d}{2}-1)^4}{\Gamma(2d-4)}, \quad (3.2a)$$

$$M_{3,2} = \int_{\mathbf{q}_1,\mathbf{q}_2,\mathbf{q}_3}\frac{1}{\mathbf{q}_1^2\mathbf{q}_3^2(\mathbf{q}_1-\mathbf{q}_2)^2(\mathbf{q}_2+\mathbf{q}_3)^2(\mathbf{q}_2+\mathbf{p})^2} = \frac{|\mathbf{p}|^{-10+3d}}{(4\pi)^{\frac{3d}{2}}}\frac{\Gamma(3-d)\Gamma(2-\frac{d}{2})\Gamma(\frac{d}{2}-1)^5}{\Gamma(d-2)\Gamma(\frac{3d}{2}-3)}, \quad (3.2b)$$

$$M_{3,3} = \int_{\mathbf{q}_1,\mathbf{q}_2,\mathbf{q}_3}\frac{1}{\mathbf{q}_1^2\mathbf{q}_3^2(\mathbf{q}_1-\mathbf{q}_2)^2(\mathbf{q}_2+\mathbf{p})^2(\mathbf{q}_3-\mathbf{p})^2} = \frac{|\mathbf{p}|^{-10+3d}}{(4\pi)^{\frac{3d}{2}}}\frac{\Gamma(5-\frac{3d}{2})\Gamma(2-\frac{d}{2})^2\Gamma(\frac{d}{2}-1)^5\Gamma(\frac{3d}{2}-4)}{\Gamma(4-d)\Gamma(d-2)^2\Gamma(2d-5)}, \quad (3.2c)$$

where the final integration over the total exchanged momenta, $\mathbf{p}$, results in a Fourier transform producing the expected $1/r^n$-type potential. To obtain the final result we must also include corrections to the kinetic term,

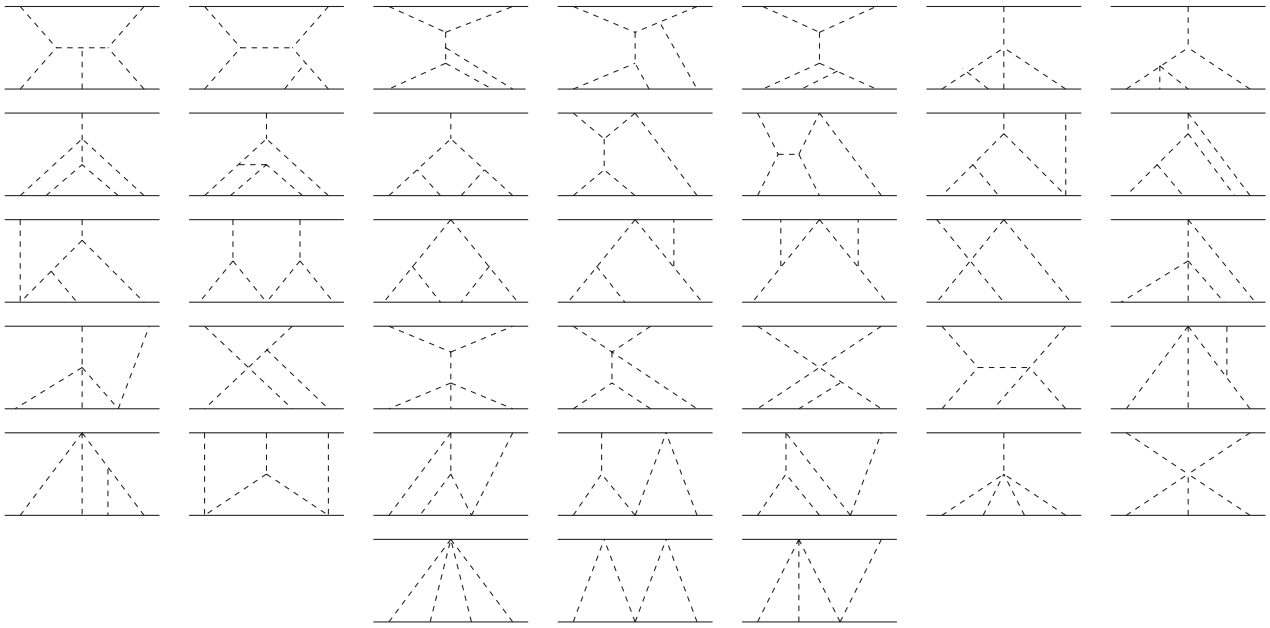

FIG. 1. Topologies at $\mathcal{O}(G^4)$ for the 3PN conservative dynamics (mirror images are omitted).

$$K(t) = \sum_{a=1,2} m_a \left(\frac{1}{2}\mathbf{v}_a^2 + \frac{1}{8}\mathbf{v}_a^4 + \frac{1}{16}\mathbf{v}_a^6 + \frac{5}{128}\mathbf{v}_a^8 + \mathcal{O}(\mathbf{v}^{10}) \right). \tag{3.3}$$

As it is well known, the potential features a divergent term, entering as a pole in the $d \to 3$ limit [25]. Following [16,22], we introduce an arbitrary regularization scale μ, associated with a d dimensional Newton's constant $G \to \mu^{d-3}G$. We display below only the part stemming off of the $1/(d-3)$ pole,

$$\begin{aligned}\mathcal{L}_{\rm 3PN}^{\rm (pole)} =& \frac{G^4 m_1 m_2}{3r^4}[m_1^3 + m_2^3 + 7m_1 m_2(m_1+m_2)]\left(\frac{1}{d-3} - 2Log(\mu_s^2 r^2)\right) \\ &+ \frac{G^3 m_1 m_2}{18 r^3}\left(\frac{2}{d-3} - 3Log(\mu_s^2 r^2)\right)\{[21m_1^2 + 24 m_1 m_2 + 5m_2^2] r(\mathbf{n}\cdot\mathbf{a}_1) - 2m_2[12m_1 + 13m_2] r(\mathbf{n}\cdot\mathbf{a}_2) \\ &+ [3m_1^2 - 24 m_1 m_2 - 2m_2^2](3(\mathbf{n}\cdot\mathbf{v}_1)^2 + 3(\mathbf{n}\cdot\mathbf{v}_2)^2 - \mathbf{v}_1^2 - \mathbf{v}_2^2 - 6(\mathbf{n}\cdot\mathbf{v}_1)(\mathbf{n}\cdot\mathbf{v}_2) + 2(\mathbf{v}_1\cdot\mathbf{v}_2))\},\end{aligned} \tag{3.4}$$

where $\mu_s \equiv \sqrt{4\pi} e^{\frac{\gamma_E}{2}} \mu$ [42], with γ_E being the Euler-Mascheroni constant. The expression for the full Lagrangian is given in the ancillary file, together with the equations of motion for both compact objects, as well as in the center-of-mass.

Similarly to the procedure outlined in [10,25], both the divergence and logarithm can be removed by a coordinate shift, in our case,

$$\mathbf{x}_1^i \to \mathbf{x}_1^i - \frac{G^3 m_2(7m_1^2 + m_2^2)}{6r^3}\left(-\frac{2}{d-3} + 3Log(\mu_s^2 r^2)\right)\mathbf{r}^i - \frac{G^2 m_1^2}{6}\left(-\frac{2}{d-3} + 2Log(\mu_s^2 r^2)\right)\mathbf{a}_1^i, \tag{3.5a}$$

$$\mathbf{x}_2^i \to \mathbf{x}_2^i + \frac{G^3 m_1(7m_2^2 + m_1^2)}{6r^3}\left(-\frac{2}{d-3} + 3Log(\mu_s^2 r^2)\right)\mathbf{r}^i - \frac{G^2 m_2^2}{6}\left(-\frac{2}{d-3} + 2Log(\mu_s^2 r^2)\right)\mathbf{a}_2^i, \tag{3.5b}$$

implemented into the leading order Lagrangian, yielding a finite result. For instance, the equations of motion in the center-of-mass frame take the form,

$$
\begin{aligned}
\mathbf{a}^i_{\rm 3PN}(\mathbf{r},\mathbf{v}) = &\left\{\frac{G^4M^4\nu}{16r^6}(2164-41\pi^2+568\nu)\right.\\
&-\frac{G^3M^3}{192r^5}[(-9024+5(-248+81\pi^2)\nu+264\nu^2-1344\nu^3)(\mathbf{n}\cdot\mathbf{v})^2+(1920+(5864-81\pi^2)\nu+192\nu^3)\mathbf{v}^2]\\
&+\frac{G^2M^2\nu}{4r^4}[2(2+69\nu+60\nu^2)(\mathbf{n}\cdot\mathbf{v})^4-4(15+16\nu+20\nu^2)(\mathbf{n}\cdot\mathbf{v})^2\mathbf{v}^2+(21-32\nu+40\nu^2)\mathbf{v}^4]\\
&+\frac{GM\nu}{16r^3}[35(1-5\nu+5\nu^2)(\mathbf{n}\cdot\mathbf{v})^6-30(4-18\nu+17\nu^2)(\mathbf{n}\cdot\mathbf{v})^4\mathbf{v}^2\\
&\left.+6(20-79\nu+60\nu^2)(\mathbf{n}\cdot\mathbf{v})^2\mathbf{v}^4-4(11-49\nu+52\nu^2)\mathbf{v}^6]\right\}\mathbf{r}^i\\
&+\left\{\frac{G^3M^3}{96r^4}(-3456+(8092+81\pi^2)\nu-2400\nu^2-768\nu^3)(\mathbf{n}\cdot\mathbf{v})\right.\\
&+\frac{G^2M^2\nu}{6r^3}[(407-177\nu-108\nu^2)(\mathbf{n}\cdot\mathbf{v})^3+6(-49+27\nu+10\nu^2)(\mathbf{n}\cdot\mathbf{v})\mathbf{v}^2]\\
&-\frac{GM\nu}{8r^2}[15(-3+8\nu+2\nu^2)(\mathbf{n}\cdot\mathbf{v})^5-6(-16+37\nu+16\nu^2)(\mathbf{n}\cdot\mathbf{v})^3\mathbf{v}^2]\\
&\left.+(-65+152\nu+48\nu^2)(\mathbf{n}\cdot\mathbf{v})\mathbf{v}^4\right\}\mathbf{v}^i,
\end{aligned}
\tag{3.6}
$$

with lower-order equations of motion substitutions and center-of-mass corrections. The above acceleration can be shown to be equivalent (upon coordinate transformations) to the known expressions in [10,25].

It is straightforward to derive the corresponding EFT Hamiltonian, via a Legendre transformation

$$
\mathcal{H}=\sum_{a=1,2} v^i_a\left(\frac{\partial\mathcal{L}}{\partial v^i_a}\right)+a^i_a\left(\frac{\partial\mathcal{L}}{\partial a^i_a}\right)+\dot{a}^i_a\left(\frac{\partial\mathcal{L}}{\partial \dot{a}^i_a}\right)-v^i_a\left(\partial_t\frac{\partial\mathcal{L}}{\partial a^i_a}\right)-a^i_a\left(\partial_t\frac{\partial\mathcal{L}}{\partial \dot{a}^i_a}\right)+v^i_a\left(\partial_t^2\frac{\partial\mathcal{L}}{\partial \dot{a}^i_a}\right)-\mathcal{L}(\mathbf{r},\mathbf{v}_1,\mathbf{a}_1,\dot{\mathbf{a}}_1,\mathbf{v}_2,\mathbf{a}_2,\dot{\mathbf{a}}_2). \tag{3.7}
$$

We limit ourselves here to the center-of-mass frame, resulting in

$$
\begin{aligned}
\mathcal{H}_{\rm 3PN}(\mathbf{r},\mathbf{v}) = &-\frac{G^4M^5\nu}{72r^4}[(36\pi^2-991)\nu+309]\\
&+\frac{G^3M^4\nu}{576r^3}[3(-480+(2296-81\pi^2)\nu+2448\nu^2+672\nu^3)(\mathbf{n}\cdot\mathbf{v})^2\\
&+(912+(-2296+81\pi^2)\nu-3024\nu^2+288\nu^3)\mathbf{v}^2]\\
&+\frac{G^2M^3\nu}{48r^2}[\nu(-91+492\nu+288\nu^2)(\mathbf{n}\cdot\mathbf{v})^4-3(84-696\nu+815\nu^2+324\nu^3)(\mathbf{n}\cdot\mathbf{v})^2\mathbf{v}^2\\
&+3(183-498\nu+406\nu^2-108\nu^3)\mathbf{v}^4]\\
&+\frac{GM^2\nu}{16r}[5\nu(1-5\nu+5\nu^2)(\mathbf{n}\cdot\mathbf{v})^6-3\nu(3-28\nu+55\nu^2)(\mathbf{n}\cdot\mathbf{v})^4\mathbf{v}^2\\
&+3\nu(-7-25\nu+125\nu^2)(\mathbf{n}\cdot\mathbf{v})^2\mathbf{v}^4+(55-215\nu+116\nu^2+325\nu^3)\mathbf{v}^6]\\
&-\frac{7M\nu}{128}(-5+59\nu-238\nu^2+323\nu^3)\mathbf{v}^8.
\end{aligned}
\tag{3.8}
$$

From here we obtain the (gauge-invariant) binding energy for quasicircular orbits to 3PN order,

$$
\begin{aligned}
E_{\rm circ} = -\frac{M\nu x}{2}&\left\{1+\left(-\frac{3}{4}-\frac{\nu}{12}\right)x+\left(-\frac{27}{8}+\frac{19}{8}\nu-\frac{\nu^2}{24}\right)x^2\right.\\
&\left.+\left[-\frac{675}{64}+\left(\frac{34445}{576}-\frac{205\pi^2}{96}\right)\nu-\frac{155}{96}\nu^2-\frac{35}{5184}\nu^3\right]x^3+\mathcal{O}(x^4)\right\},
\end{aligned}
\tag{3.9}
$$

in terms of the PN parameter $x \equiv (GM\omega)^{2/3}$, with ω the orbital frequency. As expected, this result agrees with the value given in [12,25,51].

IV. RADIATIVE DYNAMICS AT N^{3}LO

We now move onto the novel aspects of the work and the derivation of gravitational radiation at 3PN order. As shown in [22], UV divergences emerge in the derivation of the "tail-of-tail" effect, which anticipate the existence of similar UV poles in the matching of the quadrupole moment. This is expected, since the UV pole must cancel out in a full theory computation.[3] Because of this, it is vital to conduct a multipole expansion of the effective action in d dimensions, so that moments of the stress-energy tensor must be decomposed into irreducible tensors under SO(d). As shown in [55], the key contribution to the mass quadrupole moment at 3PN order becomes

$$\begin{aligned} I^{ij}_{\rm 3PN} = &\left[\int \mathrm{d}^3\mathbf{x} T^{00}_{\rm 3PN}\mathbf{x}^i\mathbf{x}^j\right]_{\rm TF} + (1-(d-3))\left[\int \mathrm{d}^3\mathbf{x} T^{aa}_{\rm 2PN}\mathbf{x}^i\mathbf{x}^j\right]_{\rm TF} - \left(\frac{4}{3}-\frac{10}{9}(d-3)\right)\left[\int \mathrm{d}^3\mathbf{x}\partial_t\tilde{T}^0_{\rm 2PN}\mathbf{x}^i\mathbf{x}^j\right]_{\rm TF} \\ &+ \left(\frac{1}{6}-\frac{13}{72}(d-3)\right)\left[\int \mathrm{d}^3\mathbf{x}\partial_t^2\tilde{T}_{\rm 1PN}\mathbf{x}^i\mathbf{x}^j\right]_{\rm TF} + \left(\frac{11}{42}-\frac{173}{882}(d-3)\right)\left[\int \mathrm{d}^3\mathbf{x}\partial_t^2 T^{00}_{\rm 2PN} r^2\mathbf{x}^i\mathbf{x}^j\right]_{\rm TF} \\ &+ \left(\frac{2}{21}-\frac{391}{3528}(d-3)\right)\left[\int \mathrm{d}^3\mathbf{x}\partial_t^2 T^{kk}_{\rm 1PN} r^2\mathbf{x}^i\mathbf{x}^j\right]_{\rm TF} - \frac{1}{7}\left[\int \mathrm{d}^3\mathbf{x}\partial_t^3\tilde{T}^0_{\rm 1PN} r^2\mathbf{x}^i\mathbf{x}^j\right]_{\rm TF} \\ &+ \frac{1}{84}\left[\int \mathrm{d}^3\mathbf{x}\partial_t^4\tilde{T}_{\rm 0PN} r^2\mathbf{x}^i\mathbf{x}^j\right]_{\rm TF} + \frac{23}{1512}\left[\int \mathrm{d}^3\mathbf{x}\partial_t^4 T^{00}_{\rm 1PN} r^4\mathbf{x}^i\mathbf{x}^j\right]_{\rm TF} + \frac{5}{1512}\left[\int \mathrm{d}^3\mathbf{x}\partial_t^4 T^{aa}_{\rm 0PN} r^4\mathbf{x}^i\mathbf{x}^j\right]_{\rm TF} \\ &- \frac{1}{189}\left[\int \mathrm{d}^3\mathbf{x}\partial_t^5\tilde{T}^0_{0PN} r^4\mathbf{x}^i\mathbf{x}^j\right]_{\rm TF} + \frac{13}{33264}\left[\int \mathrm{d}^3\mathbf{x}\partial_t^6 T^{00}_{\rm 0PN} r^6\mathbf{x}^i\mathbf{x}^j\right]_{\rm TF} \\ &+ \text{lower order corrections}, \end{aligned} \tag{4.1}$$

where $T^{ab}_{\rm nPN}$ corresponds to the nPN order in the matching of the stress-energy tensor and, for simplicity, we have used the shorthanded notation $\tilde{T}^0 \equiv T^{0k}x^k$, $\tilde{T} \equiv T^{k\ell}x^k x^\ell$. The expressions for the lower order corrections to the quadrupole moments, $I^{ij}_{\rm 1PN}$ and $I^{ij}_{\rm 2PN}$, in terms of moments of the stress-energy tensor can be found in [22,49], and must be evaluated using the equations of motion up to the 2PN order, starting from $a_{\rm N}$ (the Newtonian acceleration), which must be also evaluated in d dimensions,

$$\mathbf{a}^i_{\rm N}(\mathbf{r}) = -\frac{GM}{r^3}\left\{1+\frac{d-3}{2}[3-\mathrm{Log}(\mu_s^2 r^2)]\right\}\mathbf{r}^i. \tag{4.2}$$

In order to obtain the moments needed in (4.1) it is useful to introduce the mixed Fourier transform, $T^{\mu\nu}(t,\mathbf{k})$ introduced in [22], and expand in the long-wavelength approximation, in powers of $(\mathbf{k}\cdot\mathbf{x}) \sim \mathbf{v} \ll 1$, such that

$$\begin{aligned} T^{\mu\nu}(t,\mathbf{k}) = &\sum_{n=0}^{\infty}\frac{(-i)^n}{n!}\left(\int \mathrm{d}^3\mathbf{x} T^{\mu\nu}(t,\mathbf{x})\mathbf{x}^{i_1}\mathbf{x}^{i_2}\ldots\mathbf{x}^{i_n}\right) \\ &\times \mathbf{k}^{i_1}\mathbf{k}^{i_2}\ldots\mathbf{k}^{i_n}, \end{aligned} \tag{4.3}$$

[3]IR divergences are also present, but these either cancel in the derivation of the final observable or can be reabsorbed into a phase/time redefinition, e.g., [34].

The topologies needed to obtain the stress-energy tensor, beyond those discussed in [49], are shown in Fig. 2. The list of vertices expressing the couplings between worldlines, potential and radiation modes is detailed in Appendix B 2.

As discussed in [16,22], in the matching computation we encounter couplings between potential and radiation modes, in which the momenta of some of the potential line(s) does not scale homogeneously with the velocity. To solve this problem, it is then customary to expand the propagator in terms of the radiation momentum, as

$$\begin{aligned} \frac{1}{(\mathbf{q}+\mathbf{k})^2} = &\frac{1}{\mathbf{q}^2} - \frac{2\mathbf{q}\cdot\mathbf{k}}{\mathbf{q}^4} - \frac{\mathbf{k}^2}{\mathbf{q}^4} + \frac{4(\mathbf{q}\cdot\mathbf{k})^3}{\mathbf{q}^6} + \frac{4\mathbf{k}^2(\mathbf{q}\cdot\mathbf{k})}{\mathbf{q}^6} \\ &- \frac{8(\mathbf{q}\cdot\mathbf{k})^3}{\mathbf{q}^8} + \cdots. \end{aligned} \tag{4.4}$$

It is worth noticing that the expansion in (4.4) mixes the *internal* (potential) and *external* (radiation) momenta. As a result, the construction of the integrand often requires a tensor reduction. Similarly to the conservative case, all the resulting (two-loop) Feynman scalar integrals can be reduced to master integrals by employing IBPs relations. In particular, for the diagrams in Fig. 2 we simply need,

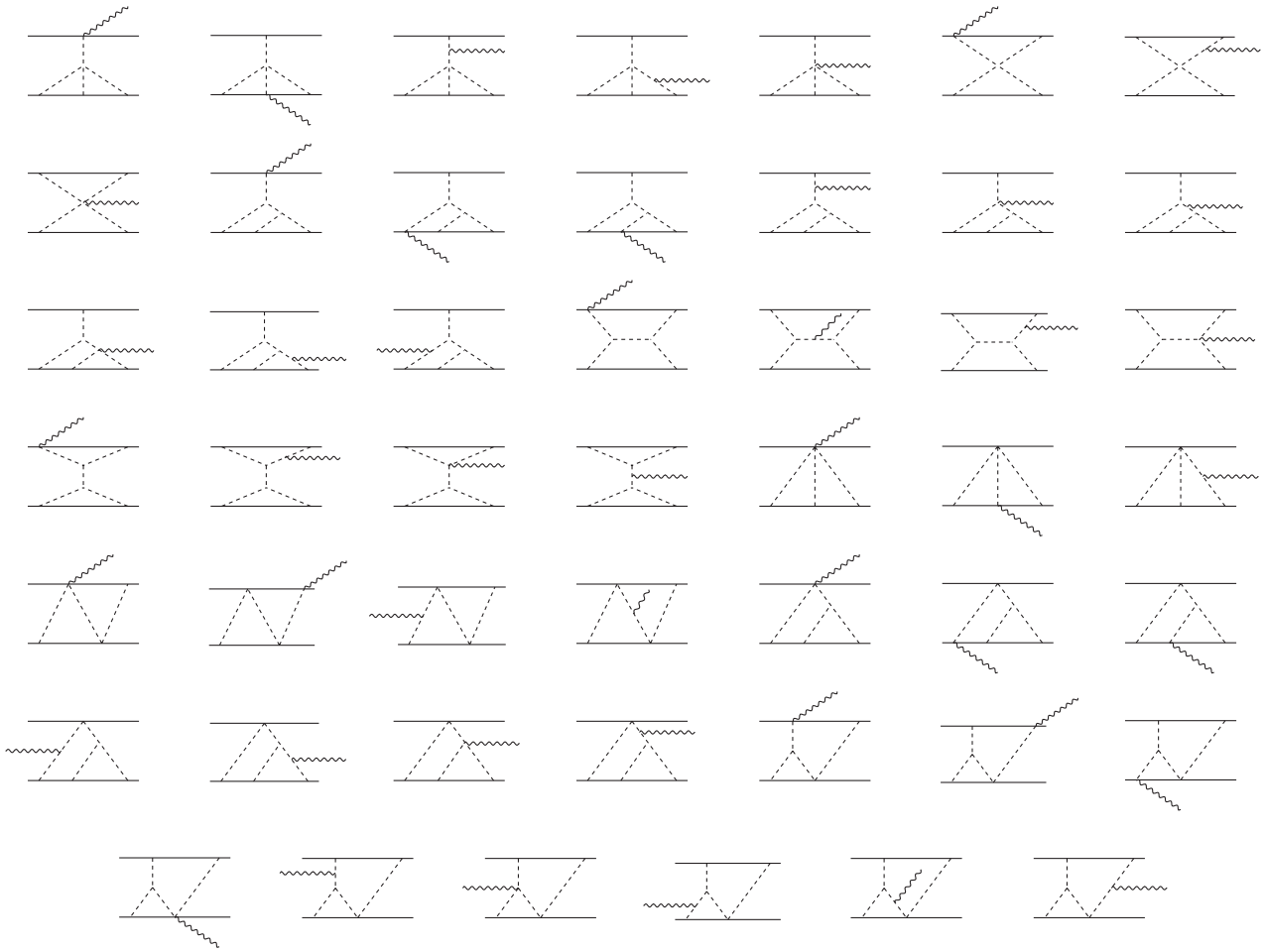

FIG. 2. Feynman topologies relevant for the matching of the stress-energy tensor. The wavy lines represents the radiation field, see also, e.g., [14,16,22,49] (mirror images are omitted).

$$M_{2,1} = \int_{\mathbf{q}_1,\mathbf{q}_2} \frac{1}{\mathbf{q}_1^2\mathbf{q}_2^2(\mathbf{q}_1+\mathbf{q}_2-\mathbf{p})^2} = \frac{|\mathbf{p}|^{-6+2d}}{(4\pi)^d}\frac{\Gamma(3-d)\Gamma(\frac{d}{2}-1)^3}{\Gamma(\frac{3d}{2}-3)}, \tag{4.5a}$$

$$M_{2,2} = \int_{\mathbf{q}_1,\mathbf{q}_2} \frac{1}{\mathbf{q}_1^2(\mathbf{q}_1+\mathbf{q}_2)^2(\mathbf{q}_1-\mathbf{p})^2(\mathbf{q}_1+\mathbf{q}_2-\mathbf{p})^2} = \frac{|\mathbf{p}|^{-8+2d}}{(4\pi)^d}\frac{\Gamma(2-\frac{d}{2})^2\Gamma(\frac{d}{2}-1)^4}{\Gamma(d-2)^2}, \tag{4.5b}$$

The computation of the remaining topologies is discussed in Appendix B 2.

Gathering all the pieces together, we obtain the contribution to the quadrupole moment to 3PN order. However, our result still depends on the original (harmonic) coordinate system. In order to be compatible with the (UV finite) result for the equations of motion from the conservative sector, we must also incorporate the coordinate shift in (3.5), which enters in the leading quadrupole moment as

$$I^{ij}_{\rm LO} \to M\nu\mathbf{r}^i\mathbf{r}^j + \frac{G^3M^4\nu}{r^3}\left\{-\nu + (1+3\nu)\left[\frac{2}{3(d-3)} - Log(\mu_s^2 r^2)\right]\right\}\mathbf{r}^i\mathbf{r}^j, \tag{4.6}$$

yielding for the quadrupole moment at 3PN the final result,

$$
\begin{aligned}
I^{ij}_{\rm 3PN}(\mathbf{r},\mathbf{v}) = \Bigg\{ & \Bigg\{ \frac{G^3M^4\nu}{1455300r^3}[(6093623 - 1050(-36181 + 1386\pi^2)\nu - 7627200\nu^2 + 2325575\nu^3)] \\
& - \frac{G^2M^3\nu}{83160r^2}[(303436 - 1296500\nu + 1674720\nu^2 + 811815\nu^3)(\mathbf{n}\cdot\mathbf{v})^2 \\
& - (646543 + 2963735\nu + 2174545\nu^2 - 1121070\nu^3)\mathbf{v}^2] \\
& + \frac{GM^2\nu}{16632r}[(336 - 10470\nu + 48957\nu^2 - 52248\nu^3)(\mathbf{n}\cdot\mathbf{v})^4 \\
& - (2271 + 11090\nu + 98311\nu^2 - 306814\nu^3)(\mathbf{n}\cdot\mathbf{v})^2\mathbf{v}^2 \\
& + 2(33156 - 188950\nu + 218411\nu^2 + 299857\nu^3)\mathbf{v}^4] \\
& + \frac{M\nu}{11088}(4561 - 55951\nu + 234134\nu^2 - 328663\nu^3)\mathbf{v}^6 \Bigg\}\mathbf{r}^i\mathbf{r}^j \\
& + \Bigg\{ \frac{G^2M^3\nu}{363825}(1957143 - 6457150\nu + 10950800\nu^2 - 4254950\nu^3) \\
& + \frac{GM^2\nu r}{4158}[3(1422 - 5807\nu + 515\nu^2 + 16490\nu^3)(\mathbf{n}\cdot\mathbf{v})^2 + (15849 - 67933\nu + 51320\nu^2 + 129781\nu^3)\mathbf{v}^2] \\
& + \frac{M\nu r^2}{5544}[20(23 - 227\nu + 718\nu^2 - 689\nu^3)(\mathbf{n}\cdot\mathbf{v})^2\mathbf{v}^2 + (1369 - 19351\nu + 90842\nu^2 - 139999\nu^3)\mathbf{v}^4] \Bigg\}\mathbf{v}^i\mathbf{v}^j \\
& + \Bigg\{ \frac{G^2M^3\nu}{41580r}(-294454 + 1287185\nu - 569730\nu^2 + 133230\nu^3)(\mathbf{n}\cdot\mathbf{v}) \\
& - \frac{GM^2\nu r}{8316}[3(-305 - 3233\nu + 8611\nu^2 + 32220\nu^3)(\mathbf{n}\cdot\mathbf{v})^3 \\
& + (34068 - 237893\nu + 376126\nu^2 + 234260\nu^3)(\mathbf{n}\cdot\mathbf{v})\mathbf{v}^2] \\
& + \frac{M\nu r}{1386}(-457 + 6103\nu - 27386\nu^2 + 40687\nu^3)(\mathbf{n}\cdot\mathbf{v})\mathbf{v}^4 \Bigg\}\mathbf{r}^i\mathbf{v}^j \\
& + \frac{107G^3M^4\nu}{105r^3}\left(\frac{2}{d-3} - 3Log(\mu_s^2r^2)\right)\mathbf{r}^i\mathbf{r}^j - \frac{214G^2M^3\nu}{105r^3}\left(\frac{1}{d-3} - Log(\mu_s^2r^2)\right)\mathbf{v}^i\mathbf{v}^j \Bigg\}_{\rm STF}. \qquad (4.7)
\end{aligned}
$$

Armed with the source multipole moments[4] we can readily derive the contribution to the GW flux via, e.g., [14],

$$
\begin{aligned}
\mathcal{P}^{\rm (inst)} = G\Bigg\{ & \frac{1}{5}I^{(3)}_{ij}I^{(3)}_{ij} + \frac{1}{189}I^{(4)}_{ijk}I^{(4)}_{ijk} + \frac{1}{9072}I^{(5)}_{ijkl}I^{(5)}_{ijkl} + \frac{1}{594000}I^{(6)}_{ijklm}I^{(6)}_{ijklm} \\
& + \frac{16}{45}J^{(3)}_{ij}J^{(3)}_{ij} + \frac{1}{84}J^{(4)}_{ijk}J^{(4)}_{ijk} + \frac{4}{14175}J^{(5)}_{ijkl}J^{(5)}_{ijkl} + \ldots \Bigg\}, \qquad (4.8)
\end{aligned}
$$

corresponding to *instantaneous* (source) terms. The expression at 3PN, evaluated in the center-of-mass, is given by

$$
\begin{aligned}
\mathcal{P}^{\rm (inst)}_{\rm 3PN}(\mathbf{r},\mathbf{v}) = & -\frac{G^7M^8\nu^2}{31185r^8}[-98457 + 361912\nu + 126798\nu^2 + 3464\nu^3] \\
& + \frac{G^6M^7\nu^2}{10914750r^7}[(4599453072 - 1925(-8448536 + 357399\pi^2)\nu + 2176410600\nu^2 - 481801600\nu^3))(\mathbf{n}\cdot\mathbf{v})^2 \\
& + (-5704087808 + 9625(-1664440 + 58401\pi^2)\nu + 563220000\nu^2 - 25902800\nu^3)\mathbf{v}^2]
\end{aligned}
$$

[4]The computation of the other necessary multipoles (needed at lower-PN order) is discussed in Appendix B 3.

$$
\begin{aligned}
&+\frac{G^5M^6\nu^2}{10914750r^6}[(-210(-134574346+15(2191804+483021\pi^2)\nu-76954850\nu^2+16506620\nu^3))(\mathbf{n}\cdot\mathbf{v})^4\\
&+6(-6326624876+1575(652462+198891\pi^2)\nu-2855456100\nu^2+694513400\nu^3)(\mathbf{n}\cdot\mathbf{v})^2\mathbf{v}^2\\
&+(10245313964-525(4720384+767151\pi^2)\nu+2731904700\nu^2-452992400\nu^3)\mathbf{v}^4]\\
&-\frac{2G^4M^5\nu^2}{51975r^5}[3(-5476951+30229425\nu-26025095\nu^2+4302385\nu^3)(\mathbf{n}\cdot\mathbf{v})^6\\
&-5(-6436413+35158037\nu-33049287\nu^2+6968200\nu^3)(\mathbf{n}\cdot\mathbf{v})^4\mathbf{v}^2\\
&+15(-1230255+6688869\nu-6699393\nu^2+1862198\nu^3)(\mathbf{n}\cdot\mathbf{v})^2\mathbf{v}^4\\
&-15(-185007+1048531\nu-955013\nu^2+378040\nu^3)\mathbf{v}^6]\\
&+\frac{G^3M^4\nu^2}{6930r^4}[5(301585+1433696\nu+1099688\nu^2-209632\nu^3)(\mathbf{n}\cdot\mathbf{v})^8\\
&+4(-1005979+5179198\nu-5288564\nu^2+1447280\nu^3)(\mathbf{n}\cdot\mathbf{v})^6\mathbf{v}^2\\
&-6(-613047+3522149\nu-4709506\nu^2+1751152\nu^3)(\mathbf{n}\cdot\mathbf{v})^4\mathbf{v}^4\\
&+4(-346489+2239826\nu-3754884\nu^2+1858800\nu^3)(\mathbf{n}\cdot\mathbf{v})^2\mathbf{v}^6]\\
&+(240945-1388854\nu+2416340\nu^2-1630560\nu^3)\mathbf{v}^8]\\
&+\frac{6848G^6M^7\nu^2}{1575r^7}\left(\frac{2}{d-3}-5Log(\mu_s^2r^2)\right)[2(\mathbf{n}\cdot\mathbf{v})^2-3\mathbf{v}^2]\\
&+\frac{3424G^5M^6\nu^2}{525r^6}\left(\frac{1}{d-3}-2Log(\mu_s^2r^2)\right)[35(\mathbf{n}\cdot\mathbf{v})^4-48(\mathbf{n}\cdot\mathbf{v})^2\mathbf{v}^2+12\mathbf{v}^4].
\end{aligned}
\tag{4.9}
$$

As anticipated, the reader will immediately notice the presence of a UV divergent term $\propto 1/(d-3)$, as well as the arbitrary renormalization scale μ_s. As we mentioned, the UV divergence and μ_s-dependence must cancel out against the hereditary contribution (from the tail-of-tail) to the (radiative) quadrupole emission. For instance, for the case of quasicircular orbits, computing the (source) GW flux using the result in (4.9), combined with the hereditary contributions (from the tail and tail-of-tail) computed in [22],[5]

$$
\begin{aligned}
\mathcal{P}^{(\mathrm{hered})}_{\mathrm{circ}}=&\frac{32\nu^2}{5G}x^5\Bigg\{4\pi x^{3/2}+\left(-\frac{8191}{672}-\frac{583}{24}\nu\right)\pi x^{5/2}\\
&+\left[\frac{455153}{11025}+\frac{16\pi^2}{3}-\frac{1712}{105}\gamma_E-\frac{856}{105}\left(\frac{1}{d-3}+4Log2-\frac{7}{3}Logx+\frac{5}{3}Log\bar{\mu}_s^2\right)\right]x^3+\mathcal{O}(x^{7/2})\Bigg\},
\end{aligned}
\tag{4.10}
$$

where $\bar{\mu}_s\equiv GM\mu_s$, we arrive at the total energy flux,

$$
\begin{aligned}
\mathcal{P}_{\mathrm{circ}}=&\mathcal{P}^{(\mathrm{inst})}_{\mathrm{circ}}+\mathcal{P}^{(\mathrm{hered})}_{\mathrm{circ}}\\
=&\frac{32\nu^2}{5G}x^5\Bigg\{1+\left(-\frac{1247}{336}-\frac{35}{12}\nu\right)x+4\pi x^{3/2}+\left(-\frac{44711}{9072}+\frac{9271}{504}\nu+\frac{65}{18}\nu^2\right)x^2+\left(-\frac{8191}{672}-\frac{583}{24}\nu\right)\pi x^{5/2}\\
&+\left[\frac{6643739519}{69854400}-\frac{1712}{105}\gamma_E+\frac{16\pi^2}{3}+\left(-\frac{134543}{7776}+\frac{41}{48}\pi^2\right)\nu\right.\\
&\left.-\frac{94403}{3024}\nu^2-\frac{775}{324}\nu^3-\frac{856}{105}Log(16x)\right]x^3+\mathcal{O}(x^{7/2})\Bigg\}.
\end{aligned}
\tag{4.11}
$$

Gladly, the above expression is not only scheme-independent and UV-finite, it is also in perfect agreement with the previous 3PN result [50,51], see also [10].

[5]Both the leading and NLO tail contribution to the flux were obtained using the tail's universal character [see Eqs. (12) and (22) in [22]], which applies to all the relevant (mass- and current-type) multipole moments. Moreover, the ("instantaneous") contributions due to memory terms, in principle at 2.5PN order, can be shown to vanish [See Eqs. (8.2) and (8.3) in [62]].

V. CONCLUSIONS

Using the EFT approach to gravitational dynamics, we computed the equations of motion and (source) multipole moments needed for the derivation of the (instantaneous) contribution to the GW flux at N^{3}LO. Upon including the hereditary corrections due to the tail and tail-of-tail effects obtained in [22], the calculations presented here provide—for the first time—an independent confirmation of the value of the GW flux for circular orbits at 3PN order derived in [50,51]. The EFT formalism readily incorporates all the relevant contributions from the "near" and "far" zones, yielding UV finite results without the need of the "ambiguity parameters" that polluted the original derivations [50–52]. Our results here illustrate, similarly to the resolution of IR ambiguities in the conservative sector at 4PN order [40–42], the usefulness of the separation of scales and matching computation introduced in [16], in conjunct with dim. reg. to handle divergent integrals (either due to the point-particle approximation and/or split into regions). Similarly to the upgrading to spin effects in the conservative sector, by simply including new worldline couplings [14,17–20,23,24,32–34], the derivations presented here pave the way to the inclusion of spin corrections in the GW flux to the same N^{3}LO level of precision, up to 5PN order, that will be presented elsewhere. We also do not foresee any obstacle to continue moving forward to higher orders, towards the present state of the art at N^{4}LO [27,28].

ACKNOWLEDGMENTS

It is a pleasure to thank François Larrouturou for several enlightening discussions, comments, and cross checks. The work of L. A. was supported by the International Helmholtz-Weizmann Research School for Multimessenger Astronomy, funded through the Initiative and Networking Fund of the Helmholtz Association. The work of R. A. P and Z. Y. was funded by the ERC-CoG "Precision Gravity: From the LHC to LISA" provided by the European Research Council under the European Union's H2020 research and innovation program (Grant Agreement No. 817791).

APPENDIX A: POST-NEWTONIAN TOOLKIT

This Appendix lists various expressions and relations previously obtained in the literature which are relevant for our computations here. The two set of topologies needed to 2PN order are shown in Figs. 3 and 4 for the conservative and radiative dynamics, respectively. The evaluation of these diagrams follows the same steps reported in the main text for the 3PN case, and only two- and one-loop master integrals are needed. While the two-loop ones are already shown in (4.5), the generalized formula for the single one-loop master integral is given by

$$M_{1,1} = \int_{\mathbf{q}_1} \frac{1}{[\mathbf{q}_1^2]^a[(\mathbf{q}_1+\mathbf{p})^2]^b} = \frac{(\mathbf{p}^2)^{\frac{d}{2}-a-b}}{(4\pi)^{\frac{d}{2}}} \frac{\Gamma(a+b-\frac{d}{2})}{\Gamma(a)\Gamma(b)} \frac{\Gamma(\frac{d}{2}-a)\Gamma(\frac{d}{2}-b)}{\Gamma(d-a-b)}. \tag{A1}$$

This formula is also used for the evaluation of (3.2) and (4.5). The final integration over the momentum transfer, $\mathbf{p}$, is always performed via the Fourier integral

$$\int_{\mathbf{p}} \frac{e^{-i\mathbf{p}\cdot\mathbf{r}}}{[\mathbf{p}^2]^a} = \frac{1}{(4\pi)^{\frac{d}{2}}} \frac{\Gamma(\frac{d}{2}-a)}{\Gamma(a)} \left(\frac{r^2}{4}\right)^{a-\frac{d}{2}}, \tag{A2}$$

which can also be used to derive tensorial expressions, e.g.,

$$\int_{\mathbf{p}} \frac{e^{-i\mathbf{p}\cdot\mathbf{r}}\mathbf{p}^i\mathbf{p}^j\mathbf{p}^\ell}{[\mathbf{p}^2]^a} = i\frac{\partial}{\partial\mathbf{r}^i} i\frac{\partial}{\partial\mathbf{r}^j} i\frac{\partial}{\partial\mathbf{r}^\ell} \int_{\mathbf{p}} \frac{e^{-i\mathbf{p}\cdot\mathbf{r}}}{[\mathbf{p}^2]^a}. \tag{A3}$$

From the equations of motion we can derive the PN corrections to the center-of-mass frame, yielding

$$\delta\mathbf{r}_{1\mathrm{PN}} = \frac{\Delta\nu}{2}\left(-\frac{GM}{r}+\mathbf{v}^2\right)\mathbf{r}, \tag{A4a}$$

$$\delta\mathbf{r}_{2\mathrm{PN}} = \Delta\nu\left\{-\frac{G^2M^2}{4r^2}(-7+2\nu)+\frac{GM}{8r}[(-1+6\nu)(\mathbf{n}\cdot\mathbf{v})^2 + (19+12\nu)\mathbf{v}^2] + \frac{3}{8}(1-4\nu)\mathbf{v}^4\right\}\mathbf{r} - \frac{7GM}{4}\Delta\nu(\mathbf{n}\cdot\mathbf{v})\mathbf{v}, \tag{A4b}$$

$$\delta\mathbf{v}_{1\mathrm{PN}} = \Delta\nu\left\{-\frac{GM}{2r^2}(\mathbf{n}\cdot\mathbf{v})\mathbf{r}+\frac{1}{2}\left[-\frac{GM}{2r}+\mathbf{v}^2\right]\mathbf{v}\right\}, \tag{A4c}$$

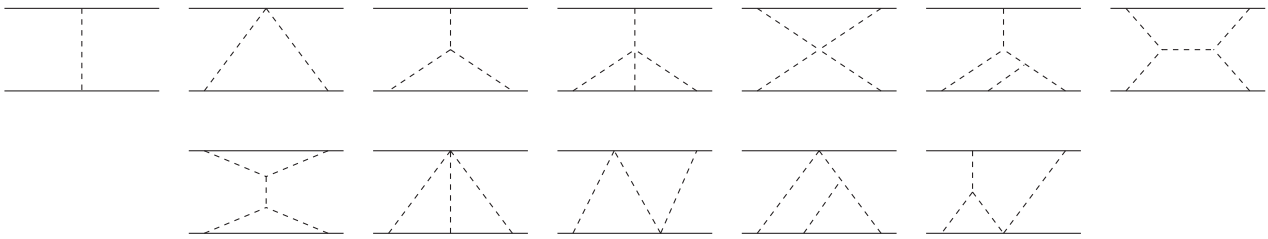

FIG. 3. Topologies needed for the gravitational potential to N^{2}LO (without mirror images).

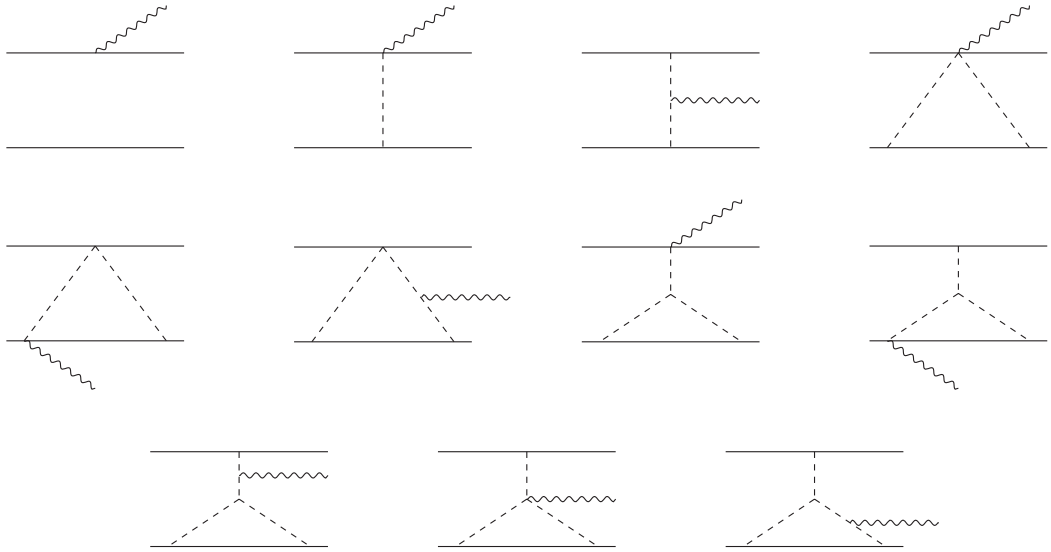

FIG. 4. Topologies needed for the radiative sector to N^{2}LO (without mirror images).

$$\delta\mathbf{v}_{\rm 2PN} = \Delta\nu\left\{-\frac{3G^2M^2}{4r^3}(3+2\nu)(\mathbf{n}\cdot\mathbf{v}) + \frac{GM}{8r^2}(\mathbf{n}\cdot\mathbf{v})[(3-6\nu)(\mathbf{n}\cdot\mathbf{v})^2+(-9+8\nu)\mathbf{v}^2]\right\}\mathbf{r} + \Delta\nu\left\{-\frac{G^2M^2}{2r^2}(-7+\nu)+\frac{GM}{8r}[(13+6\nu)(\mathbf{n}\cdot\mathbf{v})^2 + (5+12\nu)\mathbf{v}^2]+\frac{3}{8}(1-4\nu)\mathbf{v}^4\right\}\mathbf{v}, \tag{A4d}$$

which is sufficient for our purposes here.

APPENDIX B: CONTRIBUTIONS FROM LOWER-LOOP ORDERS

This Appendix provides the essential resources for calculating 3PN corrections from lower-order topologies, shown in Figs. 3 and 4.

1. Conservative sector

The vertices detailing the couplings between worldlines and potential gravitons are given by

$$S_H^{\mathbf{v}^0} = -\sum_{a=1,2}\frac{m_a}{2m_{\rm Pl}}\int {\rm d}t_a H^{00}(x_a), \tag{B1a}$$

$$S_H^{\mathbf{v}^1} = \sum_{a=1,2}\frac{m_a}{m_{\rm Pl}}\int {\rm d}t_a \mathbf{v}_a^i H^{0i}(x_a), \tag{B1b}$$

$$S_H^{\mathbf{v}^2} = -\sum_{a=1,2}\frac{m_a}{2m_{\rm Pl}}\int {\rm d}t_a\left(\frac{\mathbf{v}_a^2}{2}H^{00}(x_a)+\mathbf{v}_a^i\mathbf{v}_a^j H^{ij}(x_a)\right), \tag{B1c}$$

$$S_H^{\mathbf{v}^3} = \sum_{a=1,2}\frac{m_a}{2m_{\rm Pl}}\int {\rm d}t_a \mathbf{v}_a^2\mathbf{v}_a^i H^{0i}(x_a), \tag{B1d}$$

$$S_H^{\mathbf{v}^4} = -\sum_{a=1,2}\frac{m_a}{4m_{\rm Pl}}\int {\rm d}t_a\left(\frac{3\mathbf{v}_a^4}{4}H^{00}(x_a)+\mathbf{v}_a^2\mathbf{v}_a^i\mathbf{v}_a^j H^{ij}(x_a)\right), \tag{B1e}$$

$$S_H^{\mathbf{v}^5} = \sum_{a=1,2}\frac{3m_a}{8m_{\rm Pl}}\int {\rm d}t_a \mathbf{v}_a^4\mathbf{v}_a^i H^{0i}(x_a), \tag{B1f}$$

$$S_H^{\mathbf{v}^6} = -\sum_{a=1,2}\frac{m_a}{16m_{\rm Pl}}\int {\rm d}t_a\left(\frac{5\mathbf{v}_a^6}{2}H^{00}(x_a)+3\mathbf{v}_a^4\mathbf{v}_a^i\mathbf{v}_a^j H^{ij}(x_a)\right). \tag{B1g}$$

$$S_{H^2}^{\mathbf{v}^0} = \sum_{a=1,2}\frac{m_a}{8m_{\rm Pl}^2}\int {\rm d}t_a H^{00}(x_a)H^{00}(x_a), \tag{B2a}$$

$$S_{H^2}^{\mathbf{v}^1} = -\sum_{a=1,2}\frac{m_a}{2m_{\rm Pl}^2}\int {\rm d}t_a \mathbf{v}_a^i H^{0i}(x_a)H^{00}(x_a), \tag{B2b}$$

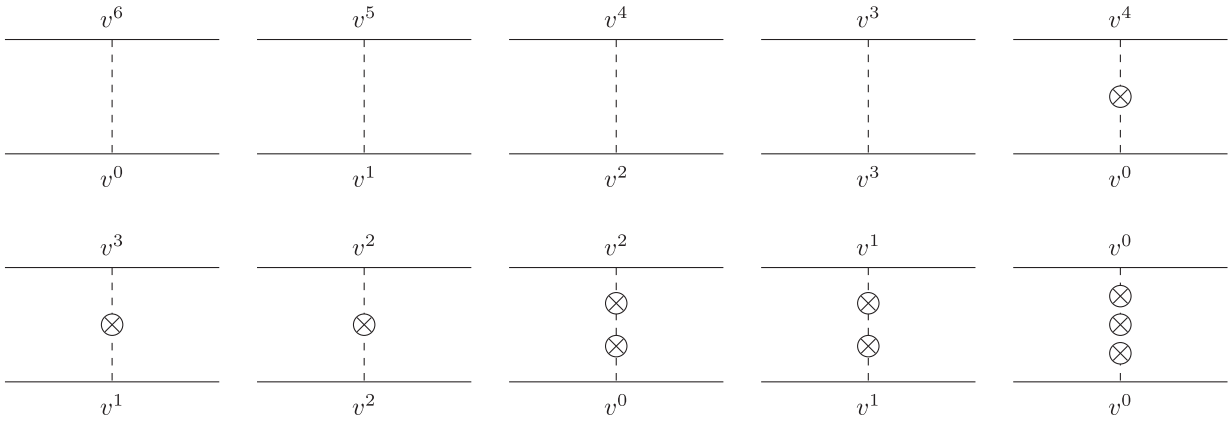

FIG. 5. Corrections due to a single-graviton exchange at 3PN.

$$S^{\mathbf{v}^2}_{H^2} = \sum_{a=1,2} \frac{m_a}{2m_{\rm Pl}^2} \int \mathrm{d}t_a \left(\frac{3\mathbf{v}_a^2}{8} H^{00}(x_a) H^{00}(x_a) + \mathbf{v}^i \mathbf{v}^j H^{0i}(x_a) H^{0j}(x_a) + \frac{1}{2} \mathbf{v}_a^i \mathbf{v}_a^j H^{ij}(x_a) H^{00}(x_a) \right), \tag{B2c}$$

$$S^{\mathbf{v}^3}_{H^2} = -\sum_{a=1,2} \frac{m_a}{2m_{\rm Pl}^2} \int \mathrm{d}t_a \left(\frac{3}{2} \mathbf{v}_a^2 \mathbf{v}_a^i H^{0i}(x_a) H^{00}(x_a) + \mathbf{v}_a^i \mathbf{v}_a^j \mathbf{v}_a^k H^{0i}(x_a) H^{ij}(x_a) \right), \tag{B2d}$$

$$\begin{aligned} S^{\mathbf{v}^4}_{H^2} = \sum_{a=1,2} \frac{m_a}{4m_{\rm Pl}^2} \int \mathrm{d}t_a \Bigg(& \frac{15\mathbf{v}_a^4}{16} H^{00}(x_a) H^{00}(x_a) + 3\mathbf{v}_a^2 \mathbf{v}^i \mathbf{v}^j H^{0i}(x_a) H^{0j}(x_a), \\ & + \frac{3}{2} \mathbf{v}_a^2 \mathbf{v}_a^i \mathbf{v}_a^j H^{ij}(x_a) H^{00} + \frac{1}{2} \mathbf{v}_a^i \mathbf{v}_a^j \mathbf{v}_a^k \mathbf{v}_a^l H^{ij}(x_a) H^{kl}(x_a) \Bigg). \end{aligned} \tag{B2e}$$

$$S^{\mathbf{v}^0}_{H^3} = -\sum_{a=1,2} \frac{m_a}{16m_{\rm Pl}^3} \int \mathrm{d}t_a H^{00}(x_a) H^{00}(x_a) H^{00}(x_a), \tag{B3a}$$

$$S^{\mathbf{v}^1}_{H^3} = \sum_{a=1,2} \frac{3m_a}{8m_{\rm Pl}^3} \int \mathrm{d}t_a \mathbf{v}_a^i H^{0i}(x_a) H^{00}(x_a) H^{00}(x_a), \tag{B3b}$$

$$\begin{aligned} S^{\mathbf{v}^2}_{H^3} = -\sum_{a=1,2} \frac{m_a}{4m_{\rm Pl}^3} \int \mathrm{d}t_a \Bigg(& \frac{5\mathbf{v}_a^2}{8} H^{00}(x_a) H^{00}(x_a) H^{00}(x_a) + 3\mathbf{v}^i \mathbf{v}^j H^{0i}(x_a) H^{0j}(x_a) H^{00}(x_a) \\ & + \frac{3}{4} \mathbf{v}_a^i \mathbf{v}_a^j H^{ij}(x_a) H^{00}(x_a) H^{00}(x_a) \Bigg). \end{aligned} \tag{B3c}$$

$$S^{\mathbf{v}^0}_{H^4} = \sum_{a=1,2} \frac{5m_a}{128m_{\rm Pl}^4} \int \mathrm{d}t_a H^{00}(x_a) H^{00}(x_a) H^{00}(x_a) H^{00}(x_a). \tag{B4}$$

The Feynman rules for gravitational self-interactions of potential modes are extracted using standard packages, and with the help of the functional derivative (in mixed Fourier space)

$$\frac{\delta H_{\alpha\beta}(t_1,\mathbf{q}_1)}{\delta H^{\mu\nu}(t_2,\mathbf{q}_2)} = \delta^{(3)}(\mathbf{q}_1+\mathbf{q}_2)\delta(t_1-t_2)I_{\mu\nu\alpha\beta}, \quad \text{(B5)}$$

where $I_{\mu\nu\alpha\beta} = \frac{1}{2}(\eta_{\mu\alpha}\eta_{\nu\beta}+\eta_{\mu\beta}\eta_{\nu\alpha})$. Each vertex is also PN expanded, depending on the number of time derivatives. The PN corrections due to the noninstantaneous nature of the binding potentials is obtained by expanding the propagator, and is represented with a cross for each insertion of a factor of $q_0^2/\mathbf{q}^2$, i.e.,

$$\frac{1}{q_0^2-\mathbf{q}^2} \simeq -\frac{1}{\mathbf{q}^2}\left[1+\frac{q_0^2}{\mathbf{q}^2}+\frac{q_0^4}{\mathbf{q}^4}+\cdots\right] \quad \text{(B6)}$$

The contributions from a mixture of non-linear gravitational effects, at various PN orders, together with non-instantaneous corrections to the propagators, are depicted in Figs. 5–7.

2. Radiative sector

Following the same logic as in the conservative sector, the worldline couplings to both potential and radiation fields are listed below,

$$S^{\mathrm{v}^0}_{H\bar{h}} = \sum_{a=1,2}\frac{m_a}{4m_{\mathrm{Pl}}^2}\int \mathrm{d}t_a H^{00}(x_a)\bar{h}^{00}(x_a), \quad \text{(B7a)}$$

$$S^{\mathrm{v}^1}_{H\bar{h}} = -\sum_{a=1,2}\frac{m_a}{2m_{\mathrm{Pl}}^2}\int \mathrm{d}t_a \mathbf{v}_a^i[H^{0i}(x_a)\bar{h}^{00}(x_a) + H^{00}(x_a)\bar{h}^{0i}(x_a)], \quad \text{(B7b)}$$

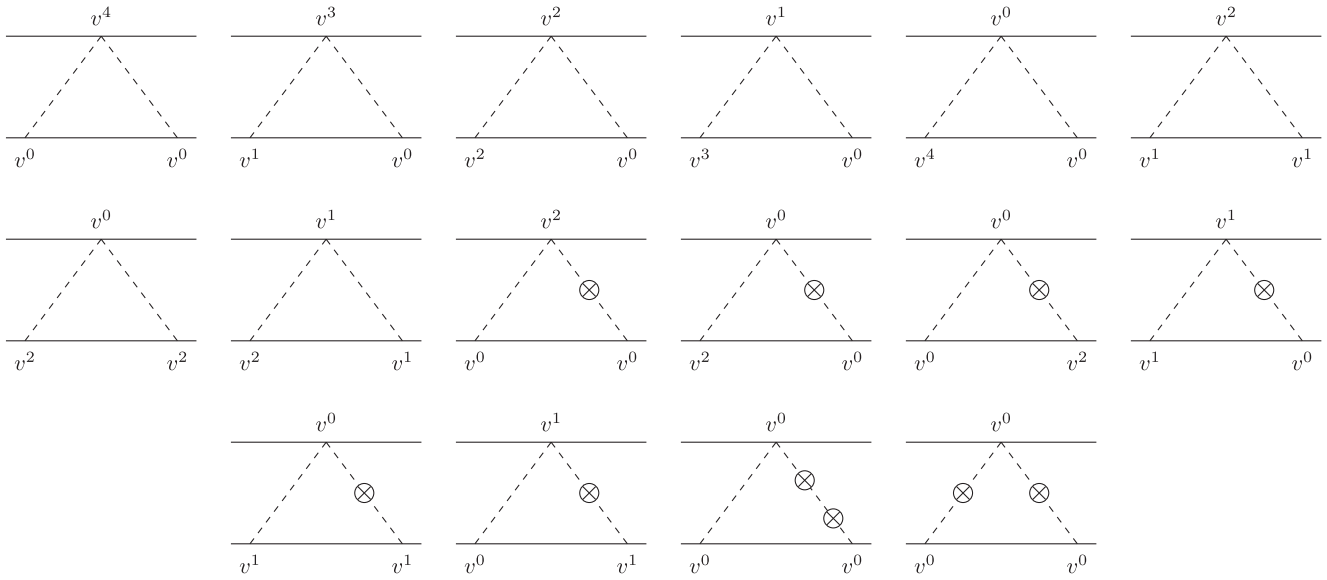

FIG. 6. Corrections due to "seagull" diagrams at 3PN.

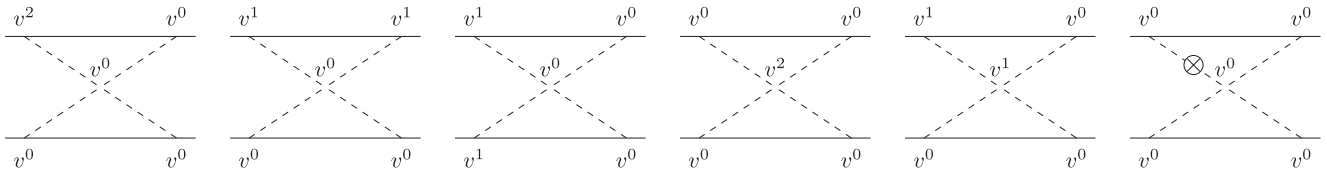

FIG. 7. Corrections due to the four-graviton vertex at 3PN.

$$S^{\mathbf{v}^2}_{H\bar{h}} = \sum_{a=1,2}\frac{m_a}{m_{\rm Pl}^2}\int \mathrm{d}t_a\left\{\frac{3\mathbf{v}_a^2}{8}H^{00}(x_a)\bar{h}^{00}(x_a) + \mathbf{v}^i\mathbf{v}^j H^{0i}(x_a)\bar{h}^{0j}(x_a) + \frac{1}{4}\mathbf{v}_a^i\mathbf{v}_a^j[H^{ij}(x_a)\bar{h}^{00}(x_a) + H^{00}(x_a)\bar{h}^{ij}(x_a)]\right\}, \tag{B7c}$$

$$S^{\mathbf{v}^3}_{H\bar{h}} = -\sum_{a=1,2}\frac{m_a}{2m_{\rm Pl}^2}\int \mathrm{d}t_a\left\{\frac{3}{2}\mathbf{v}_a^2\mathbf{v}_a^i[H^{0i}(x_a)\bar{h}^{00}(x_a) + H^{00}(x_a)\bar{h}^{0i}(x_a)] + \mathbf{v}_a^i\mathbf{v}_a^j\mathbf{v}_a^k[H^{0i}(x_a)\bar{h}^{ij}(x_a) + H^{ij}(x_a)\bar{h}^{0i}(x_a)]\right\}, \tag{B7d}$$

$$\begin{aligned}S^{\mathbf{v}^4}_{H\bar{h}} = \sum_{a=1,2}\frac{m_a}{2m_{\rm Pl}^2}\int \mathrm{d}t_a\Bigg\{&\frac{15\mathbf{v}_a^4}{16}H^{00}(x_a)\bar{h}^{00}(x_a) + 3\mathbf{v}_a^2\mathbf{v}^i\mathbf{v}^j H^{0i}(x_a)\bar{h}^{0j}(x_a), + \frac{3}{4}\mathbf{v}_a^2\mathbf{v}_a^i\mathbf{v}_a^j[H^{ij}(x_a)\bar{h}^{00} + H^{00}(x_a)\bar{h}^{ij}]\\ &+\frac{1}{2}\mathbf{v}_a^i\mathbf{v}_a^j\mathbf{v}_a^k\mathbf{v}_a^l H^{ij}(x_a)\bar{h}^{kl}(x_a)\Bigg\}.\end{aligned} \tag{B7e}$$

$$S^{\mathbf{v}^0}_{H^2\bar{h}} = -\sum_{a=1,2}\frac{3m_a}{16m_{\rm Pl}^3}\int \mathrm{d}t_a H^{00}(x_a)H^{00}(x_a)\bar{h}^{00}(x_a), \tag{B8a}$$

$$S^{\mathbf{v}^1}_{H^2\bar{h}} = \sum_{a=1,2}\frac{3m_a}{4m_{\rm Pl}^3}\int \mathrm{d}t_a \mathbf{v}_a^i[H^{0i}(x_a)H^{00}(x_a)\bar{h}^{00}(x_a) + \frac{1}{2}H^{00}(x_a)H^{00}(x_a)\bar{h}^{0i}(x_a)], \tag{B8b}$$

$$\begin{aligned}S^{\mathbf{v}^2}_{H^2\bar{h}} = -\sum_{a=1,2}\frac{m_a}{2m_{\rm Pl}^3}\int \mathrm{d}t_a\Bigg\{&\frac{15\mathbf{v}_a^2}{16}H^{00}(x_a)H^{00}(x_a)\bar{h}^{00}(x_a) + 3\mathbf{v}^i\mathbf{v}^j\left[H^{00}(x_a)H^{0i}(x_a)\bar{h}^{0j}(x_a) + \frac{1}{2}H^{0i}(x_a)H^{0j}(x_a)\bar{h}^{00}(x_a)\right]\\ &+\frac{3}{4}\mathbf{v}_a^i\mathbf{v}_a^j\left[H^{ij}(x_a)H^{00}(x_a)\bar{h}^{00}(x_a) + \frac{1}{2}H^{00}(x_a)H^{00}(x_a)\bar{h}^{ij}(x_a)\right]\Bigg\}.\end{aligned} \tag{B8c}$$

$$S^{\mathbf{v}^0}_{H^3\bar{h}} = \sum_{a=1,2}\frac{5m_a}{32m_{\rm Pl}^4}\int \mathrm{d}t_a H^{00}(x_a)H^{00}(x_a)H^{00}(x_a)\bar{h}^{00}(x_a), \tag{B9}$$

The Feynamn rules are again derived with the help of (B5). The Feynman diagrams needed at NLO and N^{2}LO are shown in Figs. 8 and 9, respectively, with the corresponding PN corrections needed to 3PN order.

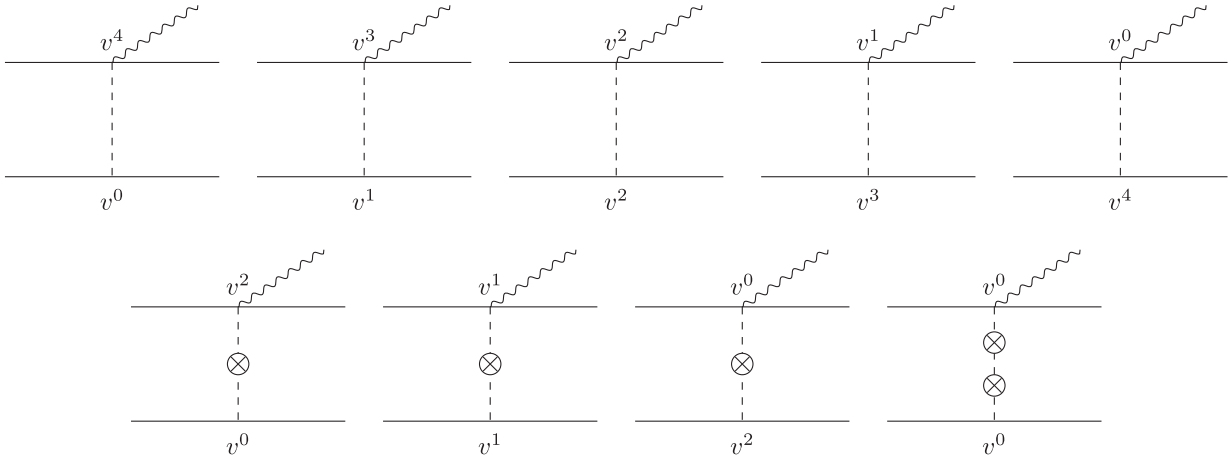

FIG. 8. Corrections due to a single-graviton exchange radiative effects at 3PN.

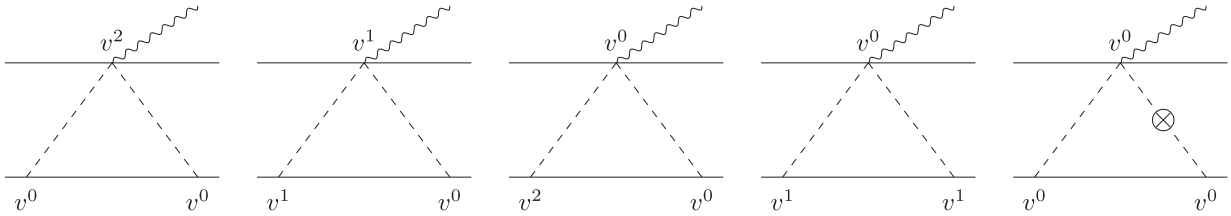

FIG. 9. Corrections due to seagull-type radiative effects at 3PN.

3. Remaining multipoles for the 3PN energy flux

In the main part of this paper we focused on the computation of the mass quadrupole at N^{3}LO. However, other multipole moments are also needed to complete the knowledge of the 3PN energy flux in (4.8). We briefly describe below the (re) derivation of the necessary multipole moments, and the comparison to analogous results available in the existing literature. See ancillary file for computer-readable expressions.

Other than the mass quadrupole, we also require the mass octupole, as well as the current quadrupole, needed to 2PN order,

$$\begin{aligned} I^{ijk}_{\rm 2PN} &= \left[\int \mathrm{d}^3\mathbf{x} T^{00}_{\rm 2PN}\mathbf{x}^i\mathbf{x}^j\mathbf{x}^k\right]_{\rm TF} + \left[\int \mathrm{d}^3\mathbf{x} T^{aa}_{\rm 1PN}\mathbf{x}^i\mathbf{x}^j\mathbf{x}^k\right]_{\rm TF} - \left[\int \mathrm{d}^3\mathbf{x}\partial_t\tilde{T}^{0}_{\rm 1PN}\mathbf{x}^i\mathbf{x}^j\mathbf{x}^k\right]_{\rm TF} \\ &+ \frac{1}{10}\left[\int \mathrm{d}^3\mathbf{x}\partial_t^2\tilde{T}_{\rm 0PN}\mathbf{x}^i\mathbf{x}^j\mathbf{x}^k\right]_{\rm TF} + \frac{1}{6}\left[\int \mathrm{d}^3\mathbf{x}\partial_t^2 T^{00}_{\rm 1PN} r^2\mathbf{x}^i\mathbf{x}^j\mathbf{x}^k\right]_{\rm TF} + \frac{1}{15}\left[\int \mathrm{d}^3\mathbf{x}\partial_t^2 T^{kk}_{\rm 0PN} r^2\mathbf{x}^i\mathbf{x}^j\mathbf{x}^k\right]_{\rm TF} \\ &- \frac{7}{90}\left[\int \mathrm{d}^3\mathbf{x}\partial_t^3\tilde{T}^{0}_{\rm 0PN} r^2\mathbf{x}^i\mathbf{x}^j\mathbf{x}^k\right]_{\rm TF} + \frac{29}{3960}\left[\int \mathrm{d}^3\mathbf{x}\partial_t^4 T^{00}_{\rm 0PN} r^4\mathbf{x}^i\mathbf{x}^j\mathbf{x}^k\right]_{\rm TF} \\ &+ \text{lower order corrections} \end{aligned} \tag{B10a}$$

$$\begin{aligned} J^{ij}_{\rm 2PN} &= \left[\int \mathrm{d}^3\mathbf{x}\varepsilon^{iba} T^{0a}_{\rm 2PN}\mathbf{x}^b\mathbf{x}^j\right]_{\rm STF} - \frac{1}{4}\left[\int \mathrm{d}^3\mathbf{x}\varepsilon^{iba}\partial_t\tilde{T}^{a}_{\rm 1PN}\mathbf{x}^b\mathbf{x}^j\right]_{\rm STF} + \frac{3}{28}\left[\int \mathrm{d}^3\mathbf{x}\varepsilon^{iba}\partial_t^2 T^{0a}_{\rm 1PN} r^2\mathbf{x}^b\mathbf{x}^j\right]_{\rm STF} \\ &- \frac{1}{56}\left[\int \mathrm{d}^3\mathbf{x}\varepsilon^{iba}\partial_t^3\tilde{T}^{a}_{\rm 0PN} r^2\mathbf{x}^b\mathbf{x}^j\right]_{\rm STF} + \frac{1}{252}\left[\int \mathrm{d}^3\mathbf{x}\varepsilon^{iba}\partial_t^4 T^{0a}_{\rm 1PN} r^4\mathbf{x}^b\mathbf{x}^j\right]_{\rm STF} \\ &+ \text{lower order corrections,} \end{aligned} \tag{B10b}$$

in terms of moments of the stress-energy tensor. Similarly to the 2PN corrections to the mass quadrupole, calculated in [49], all the relevant coefficients are extracted from the topologies shown in Fig. 4. Upon performing the matching computation, our expression for the mass octupole and current quadrupole, yield

$$\begin{aligned} I^{ijk}_{\rm 2PN}(\mathbf{r},\mathbf{v}) &= \left\{\left\{-\frac{G^2M^3\Delta\nu}{132r^2}(604-1591\nu+470\nu^2)\right.\right. \\ &+ \frac{GM^2\Delta\nu}{1320r}[(247-1593\nu+4041\nu^2)(\mathbf{n}\cdot\mathbf{v})^2+(-3853+14257\nu+17371\nu^2)\mathbf{v}^2] \\ &\left.\left.- \frac{M\Delta\nu}{1320}(771-7319\nu+16503\nu^2)\mathbf{v}^4\right\}\mathbf{r}^i\mathbf{r}^j\mathbf{r}^k\right. \\ &+ \left\{-\frac{GM^2\Delta\nu}{660}(-2461+8689\nu+4167\nu^2)(\mathbf{n}\cdot\mathbf{v}) + \frac{M\Delta\nu r}{22}(13-107\nu+204\nu^2)(\mathbf{n}\cdot\mathbf{v})\mathbf{v}^2\right\}\mathbf{r}^i\mathbf{r}^j\mathbf{v}^k \\ &+ \left\{\frac{GM^2\Delta\nu r}{330}(-1949-124\nu+2898\nu^2) + \frac{M\Delta\nu r^2}{110}[10(-1+\nu)(\mathbf{n}\cdot\mathbf{v})^2+(61-336\nu)\mathbf{v}^2]\right\}\mathbf{r}^i\mathbf{v}^j\mathbf{v}^k \\ &\left.- \frac{13M\Delta\nu r^3}{55}(1-4\nu+3\nu^2)(\mathbf{n}\cdot\mathbf{v})\mathbf{v}^i\mathbf{v}^j\mathbf{v}^k\right\}_{\rm STF}, \end{aligned} \tag{B11}$$

and

$$J^{ij}_{\rm 2PN}(\mathbf{r},\mathbf{v}) = \Big\{\Big\{-\frac{G^2M^3\Delta\nu}{504r^2}(1469-3086\nu+879\nu^2) + \frac{GM^2\Delta\nu}{504r}[(5+241\nu+1005\nu^2)(\mathbf{n}\cdot\mathbf{v})^2+(-671+2594\nu+2541\nu^2)\mathbf{v}^2] - \frac{M\Delta\nu}{336}(58-616\nu+1515\nu^2)\mathbf{v}^4\Big\}(\varepsilon^{ipq}\mathbf{r}^j+\varepsilon^{jpq}\mathbf{r}^i)\mathbf{r}^p\mathbf{v}^q + \Big\{\frac{GM^2\Delta\nu}{504}(-412-674\nu+519\nu^2)(\mathbf{n}\cdot\mathbf{v}) - \frac{25M\Delta\nu r}{336}(1-7\nu+12\nu^2)(\mathbf{n}\cdot\mathbf{v})\mathbf{v}^2\Big\}(\varepsilon^{ipq}\mathbf{v}^j+\varepsilon^{jpq}\mathbf{v}^i)\mathbf{r}^p\mathbf{v}^q\Big\}_{\rm STF}, \tag{B12}$$

in the center-of-mass frame.

As a direct cross check of these results, we compute their values for the case of circular orbits, and implement the following coordinate shift [49]

$$\mathbf{r}_{\rm EFT} \to \mathbf{r} - \frac{2G_N^2M^2}{r^2}\mathbf{r}, \tag{B13}$$

such that

$$I^{ijk} = -M\Delta\nu\Big\{1-\gamma\nu+\gamma^2\Big(-\frac{139}{330}-\frac{11923}{660}\nu-\frac{29}{110}\nu^2\Big)\Big\}[\mathbf{r}^i\mathbf{r}^j\mathbf{r}^k]_{\rm STF} - M\Delta\nu r^2\Big\{1-2\nu+\gamma\Big(\frac{1066}{165}-\frac{1433}{330}\nu+\frac{21}{55}\nu^2\Big)\Big\}[\mathbf{r}^i\mathbf{r}^j\mathbf{v}^k]_{\rm STF} \tag{B14a}$$

$$J^{ij} = -M\Delta\nu\Big\{1+\gamma\Big(\frac{67}{28}-\frac{2}{7}\nu\Big)+\gamma^2\Big(\frac{13}{9}-\frac{4651}{252}\nu-\frac{\nu^2}{168}\Big)\Big\}[\varepsilon^{ipq}\mathbf{r}^j\mathbf{r}^p\mathbf{v}^q]_{\rm STF}, \tag{B14b}$$

where we have introduced the parameter $\gamma \equiv GM/r$. These results are in perfect agreement with those displayed [10].

The derivation of the remaining (higher-order) multipoles, needed at first post-Newtonian and leading order, yields (for circular orbits)

$$I^{ijkl} = M\nu\Big\{1-3\nu+\gamma\Big(\frac{3}{110}-\frac{25}{22}\nu+\frac{69}{22}\nu^2\Big)\Big\}[\mathbf{r}^i\mathbf{r}^j\mathbf{r}^k\mathbf{r}^l]_{\rm STF} + M\nu r^2\Big\{\frac{78}{55}(1-5\nu+5\nu^2)\Big\}[\mathbf{r}^i\mathbf{r}^j\mathbf{v}^k\mathbf{v}^l]_{\rm STF} \tag{B15a}$$

$$I^{ijklm} = -M\Delta\nu(1-2\nu)[\mathbf{r}^i\mathbf{r}^j\mathbf{r}^k\mathbf{r}^l\mathbf{r}^m]_{\rm STF} \tag{B15b}$$

$$J^{ijk} = M\nu\Big\{1-3\nu+\gamma\Big(\frac{181}{90}-\frac{109}{18}\nu+\frac{13}{18}\nu^2\Big)\Big\}[\varepsilon^{ipq}\mathbf{r}^j\mathbf{r}^k\mathbf{r}^p\mathbf{v}^q]_{\rm STF} + M\nu r^2\Big\{\frac{7}{45}(1-5\nu+5\nu^2)\Big\}[\varepsilon^{ipq}\mathbf{r}^p\mathbf{v}^j\mathbf{v}^k\mathbf{v}^q]_{\rm STF} \tag{B15c}$$

$$J^{ijkm} = -M\Delta\nu(1-2\nu)[\varepsilon^{ipq}\mathbf{r}^j\mathbf{r}^k\mathbf{r}^l\mathbf{r}^p\mathbf{v}^q]_{\rm STF}, \tag{B15d}$$

also in agreement with the results in [10].

4. Consistency checks

We have also performed a few additional consistency checks. Firstly, we rederive the total mechanical energy of the system, which can be extracted from the purely temporal component of the pseudo stress-energy tensor in (4.3), at $\mathcal{O}(\mathbf{k}^0)$.

We find

$$E_{\rm 2PN}(\mathbf{r},\mathbf{v}) = \int \mathrm{d}^3\mathbf{x} T^{00}_{\rm 3PN} = -\frac{3G^3M^4\nu}{4r^3}(-2+5\nu) + \frac{G^2M^3\nu}{8r^2}[4+(-28+69\nu+12\nu^2)(\mathbf{n}\cdot\mathbf{v})^2+(30-55\nu+4\nu^2)\mathbf{v}^2]$$
$$+\frac{GM^2\nu}{8r}\{-8+3\nu(-1+3\nu)(\mathbf{n}\cdot\mathbf{v})^4+2\nu(\mathbf{n}\cdot\mathbf{v})^2[2+(1-15\nu)\mathbf{v}^2]+\mathbf{v}^2[4(3+\nu)+(21-23\nu-27\nu^2)\mathbf{v}^2]\}$$
$$+\frac{1}{16}M\nu[8+(6-18\nu)\mathbf{v}^2+5(1-7\nu+13\nu^2)\mathbf{v}^4], \tag{B16}$$

which is consistent with the 2PN corrections derived via the Legendre transformation of the Lagrangian described in (3.7).

The second self-consistent check is provided by the moment relation,

$$\int \mathrm{d}^3\mathbf{x} T^{aa}_{\rm 2PN} = \frac{1}{2}\frac{d^2}{dt^2}\int \mathrm{d}^3\mathbf{x} T^{00}_{\rm 2PN} r^2, \tag{B17}$$

Indeed, the left- and right-hand sides of the equation can be independently calculated, resulting in

$$\int \mathrm{d}^3\mathbf{x} T^{aa}_{\rm 2PN} = -\frac{G^3M^4\nu}{4r^3}(-14+15\nu)+\frac{G^2M^3\nu}{8r^2}[20+9(5+16\nu)(\mathbf{n}\cdot\mathbf{v})^2-(17+114\nu)\mathbf{v}^2]$$
$$+\frac{GM^2\nu}{8r}\{-8+3(-3+5\nu+3\nu^2)(\mathbf{n}\cdot\mathbf{v})^4+(10+15\nu-27\nu^2)\mathbf{v}^4+4\nu\mathbf{v}^2$$
$$+(\mathbf{n}\cdot\mathbf{v})^2[4(3+\nu)+(20-54\nu-30\nu^2)\mathbf{v}^2]\}$$
$$+\frac{M\nu\mathbf{v}^2}{8}[8+(4-12\nu)\mathbf{v}^2+3(1-7\nu+13\nu^2)\mathbf{v}^4], \tag{B18}$$

and

$$\frac{1}{2}\frac{d^2}{dt^2}\int \mathrm{d}^3\mathbf{x} T^{00}_{\rm 2PN} r^2 = \frac{1}{2}\frac{d^2}{dt^2}\left\{G^2M^3\nu\left\{\frac{1}{4}(67-28\nu+8\nu^2)+3\left[\frac{1}{d-3}-Log(\mu_s^2r^2)\right]\right\}\right.$$
$$+\frac{GM^2\nu r}{4}[4(4+\nu)+(-3+24\nu-10\nu^2)(\mathbf{n}\cdot\mathbf{v})^2+(17-14\nu-26\nu^2)\mathbf{v}^2]$$
$$\left.+\frac{M\nu r^2\mathbf{v}^2}{8}[4-12\nu+(3-23\nu+47\nu^2)\mathbf{v}^2]\right\}, \tag{B19}$$

respectively. It is straightforward to check that, upon taking the second-order time derivative and substituting the (d-dimensional) equations of motion, that the two expressions agree with each other.

[1] R. Abbott *et al.* (KAGRA, Virgo, and LIGO Scientific Collaborations), GWTC-3: Compact binary coalescences observed by LIGO and Virgo during the second part of the third observing run, Phys. Rev. X **13**, 041039 (2023).

[2] A. H. Nitz, S. Kumar, Y.-F. Wang, S. Kastha, S. Wu, M. Schäfer, R. Dhurkunde, and C. D. Capano, 4-OGC: Catalog of gravitational waves from compact binary mergers, Astrophys. J. **946**, 59 (2023).

[3] A. K. Mehta, S. Olsen, D. Wadekar, J. Roulet, T. Venumadhav, J. Mushkin, B. Zackay, and M. Zaldarriaga, New binary black hole mergers in the LIGO-Virgo O3b data, arXiv:2311.06061.

[4] R. Abbott *et al.* (KAGRA, Virgo, and LIGO Scientific Collaborations), Open data from the third observing run of LIGO, Virgo, KAGRA, and GEO, Astrophys. J. Suppl. Ser. **267**, 29 (2023).

[5] P. Amaro-Seoane *et al.*, Laser interferometer space antenna, arXiv:1702.00786.

[6] D. Reitze *et al.*, Cosmic Explorer: The U.S. contribution to gravitational-wave astronomy beyond LIGO, Bull. Am. Astron. Soc. **51**, 035 (2019).

[7] M. Punturo *et al.*, The Einstein Telescope: A third-generation gravitational wave observatory, Classical Quantum Gravity **27**, 194002 (2010).

[8] M. Branchesi *et al.*, Science with the Einstein Telescope: A comparison of different designs, J. Cosmol. Astropart. Phys. 07 (2023) 068.
[9] N. Afshordi *et al.* (LISA Consortium Waveform Working Group), Waveform modelling for the laser interferometer space antenna, arXiv:2311.01300.
[10] L. Blanchet, Gravitational radiation from post-Newtonian sources and inspiralling compact binaries, Living Rev. Relativity **17**, 2 (2014).
[11] A. Buonanno and B. S. Sathyaprakash, Sources of gravitational waves: Theory and observations, arXiv:1410.7832.
[12] G. Schäfer and P. Jaranowski, Hamiltonian formulation of general relativity and post-Newtonian dynamics of compact binaries, Living Rev. Relativity **21**, 7 (2018).
[13] I. Z. Rothstein, Progress in effective field theory approach to the binary inspiral problem, Gen. Relativ. Gravit. **46**, 1726 (2014).
[14] R. A. Porto, The effective field theorist's approach to gravitational dynamics, Phys. Rep. **633**, 1 (2016).
[15] W. D. Goldberger, Effective field theories of gravity and compact binary dynamics: A snowmass 2021 whitepaper, in Snowmass 2021 (2022), arXiv:2206.14249.
[16] W. D. Goldberger and I. Z. Rothstein, An effective field theory of gravity for extended objects, Phys. Rev. D **73**, 104029 (2006).
[17] R. A. Porto, Post-Newtonian corrections to the motion of spinning bodies in NRGR, Phys. Rev. D **73**, 104031 (2006).
[18] R. A. Porto and I. Z. Rothstein, The hyperfine Einstein-Infeld-Hoffmann potential, Phys. Rev. Lett. **97**, 021101 (2006).
[19] R. A. Porto and I. Z. Rothstein, Next to leading order Spin(1)Spin(1) effects in the motion of inspiralling compact binaries, Phys. Rev. D **78**, 044013 (2008); **81**, 029905(E) (2010).
[20] R. A. Porto and I. Z. Rothstein, Spin(1)Spin(2) effects in the motion of inspiralling compact binaries at third order in the post-Newtonian expansion, Phys. Rev. D **78**, 044012 (2008); **81**, 029904(E) (2010).
[21] J. B. Gilmore and A. Ross, Effective field theory calculation of second post-Newtonian binary dynamics, Phys. Rev. D **78**, 124021 (2008).
[22] W. D. Goldberger and A. Ross, Gravitational radiative corrections from effective field theory, Phys. Rev. D **81**, 124015 (2010).
[23] R. A. Porto, Next to leading order spin-orbit effects in the motion of inspiralling compact binaries, Classical Quantum Gravity **27**, 205001 (2010).
[24] R. A. Porto, A. Ross, and I. Z. Rothstein, Spin induced multipole moments for the gravitational wave flux from binary inspirals to third Post-Newtonian order, J. Cosmol. Astropart. Phys. 03 (2011) 009.
[25] S. Foffa and R. Sturani, Effective field theory calculation of conservative binary dynamics at third post-Newtonian order, Phys. Rev. D **84**, 044031 (2011).
[26] A. Ross, Multipole expansion at the level of the action, Phys. Rev. D **85**, 125033 (2012).
[27] L. Blanchet, G. Faye, Q. Henry, F. Larrouturou, and D. Trestini, Gravitational-wave phasing of quasicircular compact binary systems to the fourth-and-a-half post-Newtonian order, Phys. Rev. Lett. **131**, 121402 (2023).
[28] L. Blanchet, G. Faye, Q. Henry, F. Larrouturou, and D. Trestini, Gravitational-wave flux and quadrupole modes from quasicircular nonspinning compact binaries to the fourth post-Newtonian order, Phys. Rev. D **108**, 064041 (2023).
[29] G. Faye, S. Marsat, L. Blanchet, and B. R. Iyer, The third and a half post-Newtonian gravitational wave quadrupole mode for quasi-circular inspiralling compact binaries, Classical Quantum Gravity **29**, 175004 (2012).
[30] Q. Henry, G. Faye, and L. Blanchet, The current-type quadrupole moment and gravitational-wave mode $(\ell, m) = (2, 1)$ of compact binary systems at the third post-Newtonian order, Classical Quantum Gravity **38**, 185004 (2021).
[31] Q. Henry, Complete gravitational-waveform amplitude modes for quasicircular compact binaries to the 3.5PN order, Phys. Rev. D **107**, 044057 (2023).
[32] G. Cho, B. Pardo, and R. A. Porto, Gravitational radiation from inspiralling compact objects: Spin-spin effects completed at the next-to-leading post-Newtonian order, Phys. Rev. D **104**, 024037 (2021).
[33] G. Cho, R. A. Porto, and Z. Yang, Gravitational radiation from inspiralling compact objects: Spin effects to the fourth post-Newtonian order, Phys. Rev. D **106**, L101501 (2022).
[34] R. A. Porto, A. Ross, and I. Z. Rothstein, Spin induced multipole moments for the gravitational wave amplitude from binary inspirals to 2.5 Post-Newtonian order, J. Cosmol. Astropart. Phys. 09 (2012) 028.
[35] Q. Henry, S. Marsat, and M. Khalil, Spin contributions to the gravitational-waveform modes for spin-aligned binaries at the 3.5PN order, Phys. Rev. D **106**, 124018 (2022).
[36] Q. Henry and M. Khalil, Spin effects in gravitational waveforms and fluxes for binaries on eccentric orbits to the third post-Newtonian order, Phys. Rev. D **108**, 104016 (2023).
[37] N. T. Maia, C. R. Galley, A. K. Leibovich, and R. A. Porto, Radiation reaction for spinning bodies in effective field theory I: Spin-orbit effects, Phys. Rev. D **96**, 084064 (2017).
[38] N. T. Maia, C. R. Galley, A. K. Leibovich, and R. A. Porto, Radiation reaction for spinning bodies in effective field theory II: Spin-spin effects, Phys. Rev. D **96**, 084065 (2017).
[39] M. Levi and Z. Yin, Completing the fifth PN precision frontier via the EFT of spinning gravitating objects, J. High Energy Phys. 04 (2022) 079.
[40] C. R. Galley, A. K. Leibovich, R. A. Porto, and A. Ross, Tail effect in gravitational radiation reaction: Time nonlocality and renormalization group evolution, Phys. Rev. D **93**, 124010 (2016).
[41] R. A. Porto and I. Z. Rothstein, Apparent ambiguities in the post-Newtonian expansion for binary systems, Phys. Rev. D **96**, 024062 (2017).
[42] S. Foffa, R. A. Porto, I. Rothstein, and R. Sturani, Conservative dynamics of binary systems to fourth Post-Newtonian order in the EFT approach II: Renormalized Lagrangian, Phys. Rev. D **100**, 024048 (2019).
[43] S. Foffa and R. Sturani, Conservative dynamics of binary systems to fourth post-Newtonian order in the EFT approach I: Regularized Lagrangian, Phys. Rev. D **100**, 024047 (2019).

[44] L. Blanchet, S. Foffa, F. Larrouturou, and R. Sturani, Logarithmic tail contributions to the energy function of circular compact binaries, Phys. Rev. D **101**, 084045 (2020).
[45] G. L. Almeida, S. Foffa, and R. Sturani, Tail contributions to gravitational conservative dynamics, Phys. Rev. D **104**, 124075 (2021).
[46] G. L. Almeida, A. Müller, S. Foffa, and R. Sturani, Conservative binary dynamics from gravitational tail emission processes, Phys. Rev. D **108**, 124010 (2023).
[47] Q. Henry and F. Larrouturou, Conservative tail and failed-tail effects at the fifth post-Newtonian order, Phys. Rev. D **108**, 084048 (2023).
[48] J. Blümlein, A. Maier, P. Marquard, and G. Schäfer, The fifth-order post-Newtonian Hamiltonian dynamics of two-body systems from an effective field theory approach: Potential contributions, Nucl. Phys. **B965**, 115352 (2021).
[49] A. K. Leibovich, N. T. Maia, I. Z. Rothstein, and Z. Yang, Second post-Newtonian order radiative dynamics of inspiralling compact binaries in the effective field theory approach, Phys. Rev. D **101**, 084058 (2020).
[50] L. Blanchet, B. R. Iyer, and B. Joguet, Gravitational waves from inspiralling compact binaries: Energy flux to third post-Newtonian order, Phys. Rev. D **65**, 064005 (2002); **71**, 129903(E) (2005).
[51] L. Blanchet, T. Damour, G. Esposito-Farese, and B. R. Iyer, Gravitational radiation from inspiralling compact binaries completed at the third post-Newtonian order, Phys. Rev. Lett. **93**, 091101 (2004).
[52] L. Blanchet, G. Faye, B. R. Iyer, and B. Joguet, Gravitational wave inspiral of compact binary systems to $7/2$ post-Newtonian order, Phys. Rev. D **65**, 061501 (2002); **71**, 129902(E) (2005).
[53] L. Blanchet, T. Damour, and G. Esposito-Farese, Dimensional regularization of the third post-Newtonian dynamics of point particles in harmonic coordinates, Phys. Rev. D **69**, 124007 (2004).
[54] L. Blanchet, T. Damour, G. Esposito-Farese, and B. R. Iyer, Dimensional regularization of the third post-Newtonian gravitational wave generation from two point masses, Phys. Rev. D **71**, 124004 (2005).
[55] L. Amalberti, F. Larrouturou, and Z. Yang, Multipole expansion at the level of the action in d-dimensions, Phys. Rev. D **109**, 104027 (2024).
[56] T. Hahn, Generating Feynman diagrams and amplitudes with FeynArts 3, Comput. Phys. Commun. **140**, 418 (2001).
[57] J. M. Martín-García, xact: Efficient tensor computer algebra for the Wolfram language (2004), http://www.xact.es/.
[58] R. N. Lee, LiteRed 1.4: A powerful tool for reduction of multiloop integrals, J. Phys. Conf. Ser. **523**, 012059 (2014).
[59] See Supplemental Material at http://link.aps.org/supplemental/10.1103/PhysRevD.110.044046 for `Mathematica`-readable expressions of the various results referred to in the main text. Further details can be found in the ancillary file's header.
[60] L. Blanchet and T. Damour, Radiative gravitational fields in general relativity I. General structure of the field outside the source, Phil. Trans. R. Soc. A **320**, 379 (1986).
[61] I. Z. Rothstein, TASI lectures on effective field theories, arXiv:hep-ph/0308266.
[62] K. G. Arun, L. Blanchet, B. R. Iyer, and M. S. S. Qusailah, Inspiralling compact binaries in quasi-elliptical orbits: The complete 3PN energy flux, Phys. Rev. D **77**, 064035 (2008).